ETH
Eidgenössische Technische Hochschule Zürich
Swiss Federal Institute of Technology Zurich

Self-Organization of Pedestrians in Space and Time

Prof. Dr. rer. nat. Dirk Helbing

Chair of Sociology, in particular of Modeling and Simulation

www.soms.ethz.ch

with Anders Johansson, Wenjian Yu, Mehdi Moussaid,

Illes Farkas, Peter Molnar, Tamas Vicsek and others

Emergent Collective Behavior by Human Interactions

What interests me most about social systems is the emergence of new, functional or complex system behaviors, particularly cooperation or coordination patterns based on elementary individual interactions.

For example, lanes of uniform walking direction emerge due to self-organization.

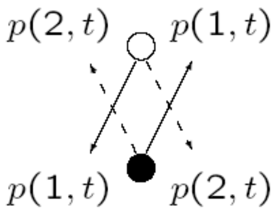

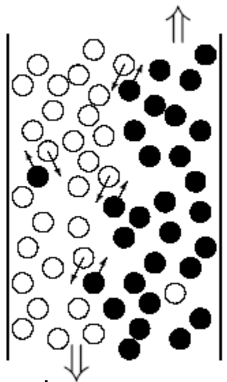

Do pedestrians behave as individuals or social beings?

Preference of right-hand side is a convention, which can be understood by evolutionary game theory, as the payoff is larger for individuals who follow the majority behavior (B. Arthur'89/A. Rapoport'93)

A Crowd as A Self-Organized System

- Repeated interactions at a local scale
- Emerging structures at a global scale
- Distributed organization

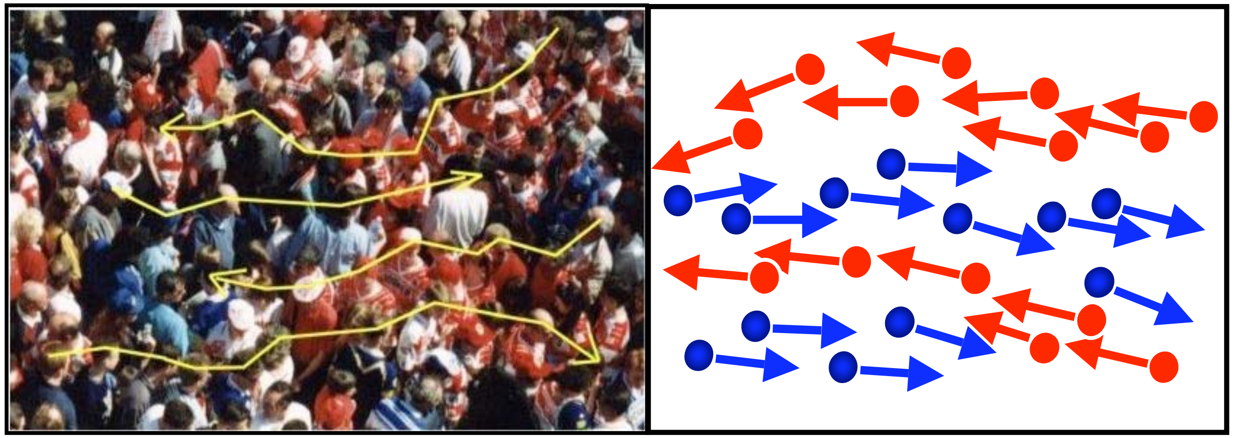

Underlying Mechanisms?

Some Analogies between Pedestrian Crowds and Fluids

- Footprints in snow look similar to streamlines of fluids.
- There are gaseous (free), fluid (obstructed), and solid (immobile) states.
- Passing through a standing pedestrian crowd leads to river-like streams.
- In pushy pedestrian crowds one can observe shock waves.
- Similarities with granular media are dominating at high pedestrians densities (e.g. mutual obstructions, occurance of force lines).

Pedestrian Models

- The dynamics of pedestrian crowds can be modeled on different levels:
  - **Microscopic** level: Molecular dynamic models or cellular automata.
  - **Mesoscopic** level: Gas-kinetic (Boltzmann-like) models.
  - **Macroscopic** level: Fluid-dynamic or queuing network models.
- For simulations, microscopic models are most appropriate because of the following difficulties:
  - Pedestrian crowds are compressible. The variation of pedestrian density is extreme.
  - Every pedestrian needs a certain space that can be relatively large in comparison with the mean interaction-free path.
  - Several flows with different directions of motion penetrate each other.
  - Pedestrian motion is anisotropic. The mobility and velocity variance into the direction of motion is larger than perpendicular to it.
  - Excluded volume and friction effects similar to granular interactions must be taken into account.

Examples of Pedestrian Models

Name	Type	Representation	Scale
Fruin (1971)	LOS Concept	Density	Discrete
Henderson (1971)	Fluiddynamic	Flow	Continuous
Predteschenski+Milinski (1971)	Planning Guidelines	Velocity	Continuous
Garbrecht (1973)	Queuing Model	Room Occupation, Evacuation Time	Discrete
Highway Capacity Manual (1985)	Regression Models	Linear Regression Formulas	Continuous
Helbing (1992)	Gas-kinetic, Fluiddynamic	Flow	Continuous
Løvas (1994)	Queuing	Pedestrians	Discrete
Helbing & Molnar (1995)	Microscopic	Pedestrians	Continuous
Still (2000)	Quasi-Microscopic, Simulated Anneal.	Pedestrians	Continuous
Hoogendoorn & Bovy (2000)	Gas-kinetic	Flow	Discrete
Hughes (2000)	Fluiddynamic	Flow	Continuous
Klüpfel, Schreckenberg et al. (2000)	Cellular Automaton	Cell Occupation	Discrete
Schadschneider (2001)	Cellular Automaton	Cell Occupation	Discrete
AlGadhi,Mahmassani et al (2001)	Microscopic	Pedestrians	Discrete

Regression Models and Design Guidelines

CROSSWALK ANALYSIS WORKSHEET

Location: *Ralph Ave. & Crossway Blvd.*

City, State: *Townsville, KY*

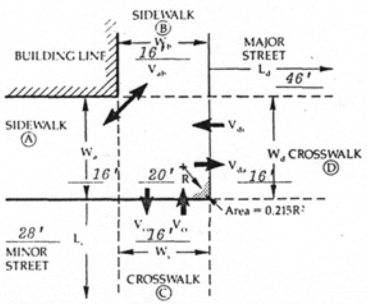

SIGNAL TIMING (sec)

C = 80
G_{mj} = 48 R_{mj} = 32
G_{mi} = 32 R_{mi} = 48

PEDESTRIAN VOLUMES

Flow	Ped/Min	Ped/Cyc
v_{ci}	36	48
v_{co}	20	27
v_{di}	30	40
v_{do}	16	21
$v_{a,b}$	15	20
v_{tot}	117	156

CROSSWALK AREAS	$A_c = L_cW_c =$	448	sq ft
	$A_d = L_dW_d =$	736	sq ft
CROSSWALK TIME-SPACE	$TS_c = A_c(G_{mj} - 3)/60 =$	336	sq ft-min
	$TS_d = A_d(G_{mi} - 3)/60 =$	356	sq ft-min
CROSSING TIMES	$t_{wc} = L_c/4.5 =$	6.2	sec
	$t_{wd} = L_d/4.5 =$	10.2	sec
CROSSWALK OCCUPANCY TIME (use ped/cycle)	$T_{wc} = (v_{ci} + v_{co})(t_{wc}/60) =$	7.8	ped-min
	$T_{wd} = (v_{di} + v_{do})(t_{wd}/60) =$	10.4	ped-min

AVERAGE PEDESTRIAN SPACE AND LOS	$M_c = TS_c/T_{wc} =$	43	sq ft/ped; LOS =	B (Table 13-3)
	$M_d = TS_d/T_{wd} =$	34	sq ft/ped; LOS =	C (Table 13-3)
MAXIMUM SURGE (use ped/min)	$V_{mc} = (v_{ci} + v_{co})(R_{mj} + 3 + t_{wc})/60 =$	38.5	ped	
	$V_{md} = (v_{di} + v_{do})(R_{mi} + 3 + t_{wd})/60 =$	46.9	ped	
SURGE PEDESTRIAN SPACE AND SURGE LOS	$M_c(Max) = A_c/V_{mc} =$	11.6	sq ft/ped; LOS =	E (Table 13-3)
	$M_d(Max) = A_d/V_{md} =$	15.7	sq ft/ped; LOS =	D (Table 13-3)

Figure 13-21. Worksheet for crosswalk analysis of sample calculation.

Classical Fundamental Diagrams

Fundamental Diagrams (Source: Ulrich Weidmann)

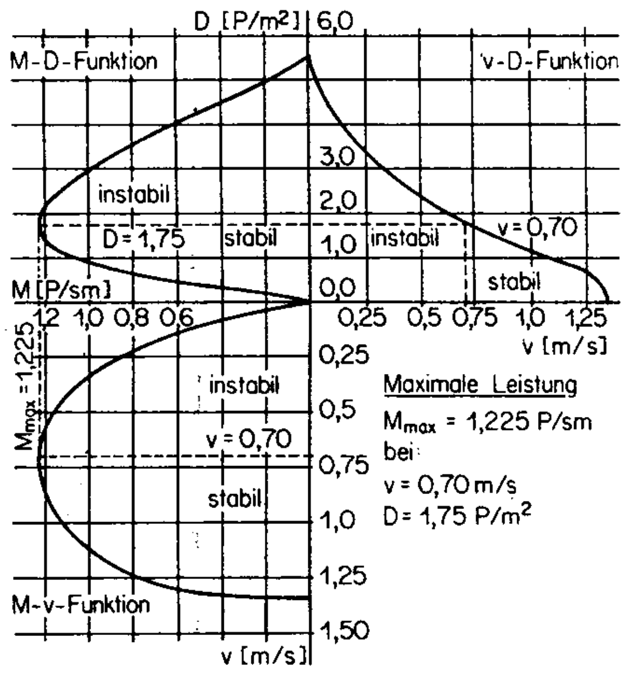

Abb. 7: Fundamentaldiagramm für Fuß-wege, Richtungsverkehr

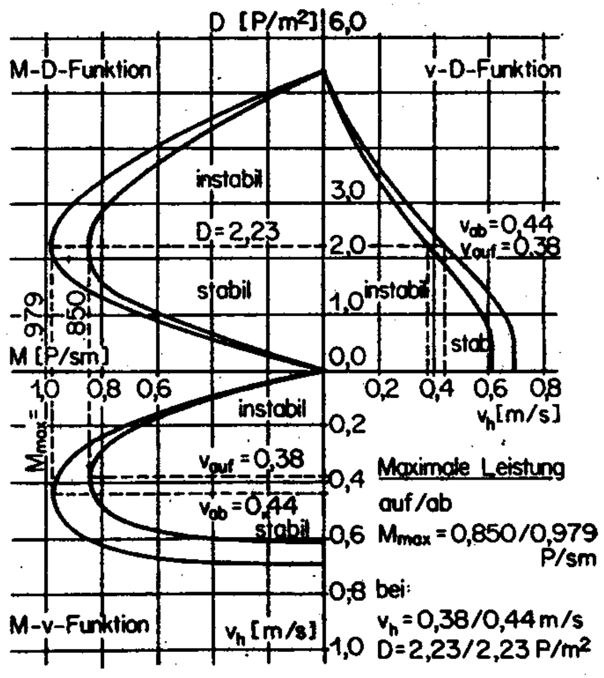

Abb. 8: Fundamentaldiagramm für Trep-pen, Richtungsverkehr

Calculations According to Predtetschenki and Milinski

Wir nehmen an, daß $f=0{,}125\ m^2$; $P=468:0{,}125=58{,}50\ m^2$ und sehen vor, daß $t_{Gr}=3{,}00$ min.
Bestimmt wird die Bewegungszeit der Personen aus Block 1 bis zum Ausgang aus dem Längsgang ($b=1{,}20$ m) entlang der Wand zur Tür (vgl. Abschn. 2.6.3.).
$R=2$ Reihen; $P_R=7$ Plätze; $P=R\cdot P_R\cdot f=2\cdot 7\cdot 0{,}125=1{,}75\ m^2$; $l_R=3{,}50$ m; $b'_R=0{,}90$ m.
Nach Tabelle ist $Q_R=4{,}47\ m^2\cdot min^{-1}$; $v_R=17{,}76\ m\cdot min^{-1}$;

$$t_R=\frac{3{,}50}{17{,}76}=0{,}20\ min.$$

Nach der Formel ergibt sich:

$$q=\frac{Q_R\cdot R}{b}=\frac{4{,}47\cdot 2}{1{,}20}=7{,}45\ m\cdot min^{-1}<q_{max}=10{,}12\ m\cdot min^{-1}.$$

Folglich stabilisiert sich die Bewegung bei $D_i=0{,}42$, was $q_i=7{,}45\ m\cdot min^{-1}$ entspricht, dann ist $q_{i,R}=q_i=7{,}45\ m\cdot min^{-1}$.

$$q_1=\frac{Q_R}{b}=\frac{4{,}47}{1{,}20}=3{,}72\ m\cdot min^{-1};\quad D_1=0{,}09;$$

$$q_2=7{,}45\ m\cdot min^{-1};\quad D_2=0{,}42;\quad D_i=D_2=0{,}42;\quad Q_2=8{,}94\ m^2\cdot min^{-1};$$

$$\sum_1^{i-1}D=D_1=0{,}09;\quad q_{i-1}=q_1=3{,}72\ m\cdot min^{-1}.$$

Nach Formel (50) ist:

$$t=\frac{b'_R}{q_{i,R}}\cdot\left[\frac{D_i}{\Delta q}\cdot(q_{i,R}-q_{i-1})+\sum_1^{i-1}D\right]+\frac{P}{q_{i,R}\cdot b}$$

$$=\frac{0{,}90}{7{,}45}\cdot\left[\frac{0{,}42}{3{,}72}\cdot(7{,}45-3{,}72)+0{,}09\right]+\frac{1{,}75}{7{,}45\cdot 1{,}20}=0{,}26\ min.$$

Bei kurzen Gängen mit geringer Anzahl von Plätzen in der Reihe sind sich t und t_R im Wert einander sehr nahe.
Berechnen wir nun die Bewegungszeit der Personen aus Block 3 bis zum Austritt aus dem Längsgang ($b=1{,}20$ m) in den Quergang, der zur Tür führt. $R=8$ Reihen, $P_R=6$ Plätze; die Reihen befinden sich zu beiden Seiten des Ganges.
$P=R\cdot P_R\cdot 2\cdot f=8\cdot 6\cdot 2\cdot 0{,}125=12{,}00\ m^2$; $l_R=3{,}00$ m; $b'_R=0{,}90$ m.

$$Q_R=4{,}47\ m^2\cdot min^{-1};\quad v_R=17{,}76\ m\cdot min^{-1};\quad t_R=\frac{l_R}{v_R}=\frac{3{,}00}{17{,}76}=0{,}17\ min;$$

$$q=\frac{2\cdot Q_R\cdot R}{1{,}20}=\frac{2\cdot 4{,}47\cdot 8}{1{,}20}=59{,}45\ m\cdot min^{-1}>q_{max}=10{,}12\ m\cdot min^{-1}.$$

In diesem Fall stabilisiert sich die Bewegung im Gang zum Zeitpunkt t_R oder bei D_{max}.

Wir überprüfen mittels t_R:

$$D_{i,R}=\frac{2\cdot Q_R}{b\cdot b'_R}\cdot t_R=\frac{2\cdot 4{,}47}{1{,}20\cdot 0{,}90}\cdot 0{,}17$$

$$=1{,}41>D=0{,}75\ \text{bei}\ q_{max}=10{,}12\ m\cdot min^{-1}.$$

Folglich stabilisiert sich der Prozeß bei D_{max}.

$$q_1=\frac{2\cdot Q_R}{b}=\frac{2\cdot 4{,}47}{1{,}20}=7{,}45\ m\cdot min^{-1};\quad D_1=0{,}42;$$

$$\Delta q=q_1=7{,}45\ m\cdot min^{-1};$$

$$q_2=14{,}90\ m\cdot min^{-1}>q_{max}=10{,}12\ m\cdot min^{-1};$$

$$D_i=D_1=0{,}42;\quad \sum_1^{i-1}D=0;\quad q_{i-1}=0.$$

Nach Formel (50) ist:

$$t=\frac{b'_R}{q_{i,R}}\cdot\left[\frac{D_i}{\Delta q}\cdot(q_{i,R}-q_{i-1})+\sum_1^{i-1}D\right]+\frac{P}{q_{i,R}\cdot b}$$

$$=\frac{0{,}90}{8{,}35}\cdot\left[\frac{0{,}42}{7{,}45}\cdot(8{,}35-0)+0\right]+\frac{12{,}00}{8{,}35\cdot 1{,}20}=1{,}22\ min.$$

Nur im ersten Moment beim Austritt in den Quergang wird der Personenstrom die Dichte $D_1=0{,}42$, aber gleich danach $D_{max}=0{,}92$ haben. Diese Dichte kann für die Berechnung angewendet werden. Anschließend führen wir die Berechnung der Bewegungsparameter am Block A durch (im Quergang des Saales, der zur Tür führt, ist $b=1{,}20$; $P=13\cdot 0{,}125=1{,}63\ m^2$). Vom Zeitpunkt des Beginns der Evakuierung befinden sich die Menschen sofort im Gang in seiner ganzen Länge, die Dichte des Stromes wird:

$$D=\frac{P}{b\cdot l}=\frac{1{,}63}{1{,}20\cdot 6{,}50}=0{,}21;$$

$v=27{,}27\ m\cdot min^{-1}$; $q=5{,}73\ m\cdot min^{-1}$; $Q=6{,}88\ m^2\cdot min^{-1}$.
Die aus den Blöcken 1, 3 und A kommenden Personen vereinigen sich zu einem Strom. Die Grafik (s. Abb. 93) spiegelt die Bewegung im Quergang wider.
Nun wird der Verkehrsweg bestimmt (vgl. Skizze an der linken Seite der Abb. 93). Vom Augenblick des Beginns der Evakuierung an befindet sich im Quergang der Personenstrom aus Block A, und zum Endteil dieses Stromes kommt der Kopfteil des Stromes aus Block 3. Folglich wird ihre Umformierung nach dem Schema $v_1>v_2$ stattfinden. Dann wird die Geschwindigkeit der Umformierung

$$v'=\frac{q_2-q_1}{D_2-D_1}=\frac{8{,}35-5{,}73}{0{,}92-0{,}21}=3{,}69\ m\cdot min^{-1}.$$

Nun tragen wir in die Grafik die Linien der Bewegung des Kopfteiles des Stromes von Block A ($v=27{,}27\ m\cdot min^{-1}$), die Linie der Umformierung ($v'=3{,}69\ m\cdot min^{-1}$) und die Linie der Bewegung des Stromendes aus Block 3 im Quergang ein

Example: Evacuation of a Cinema

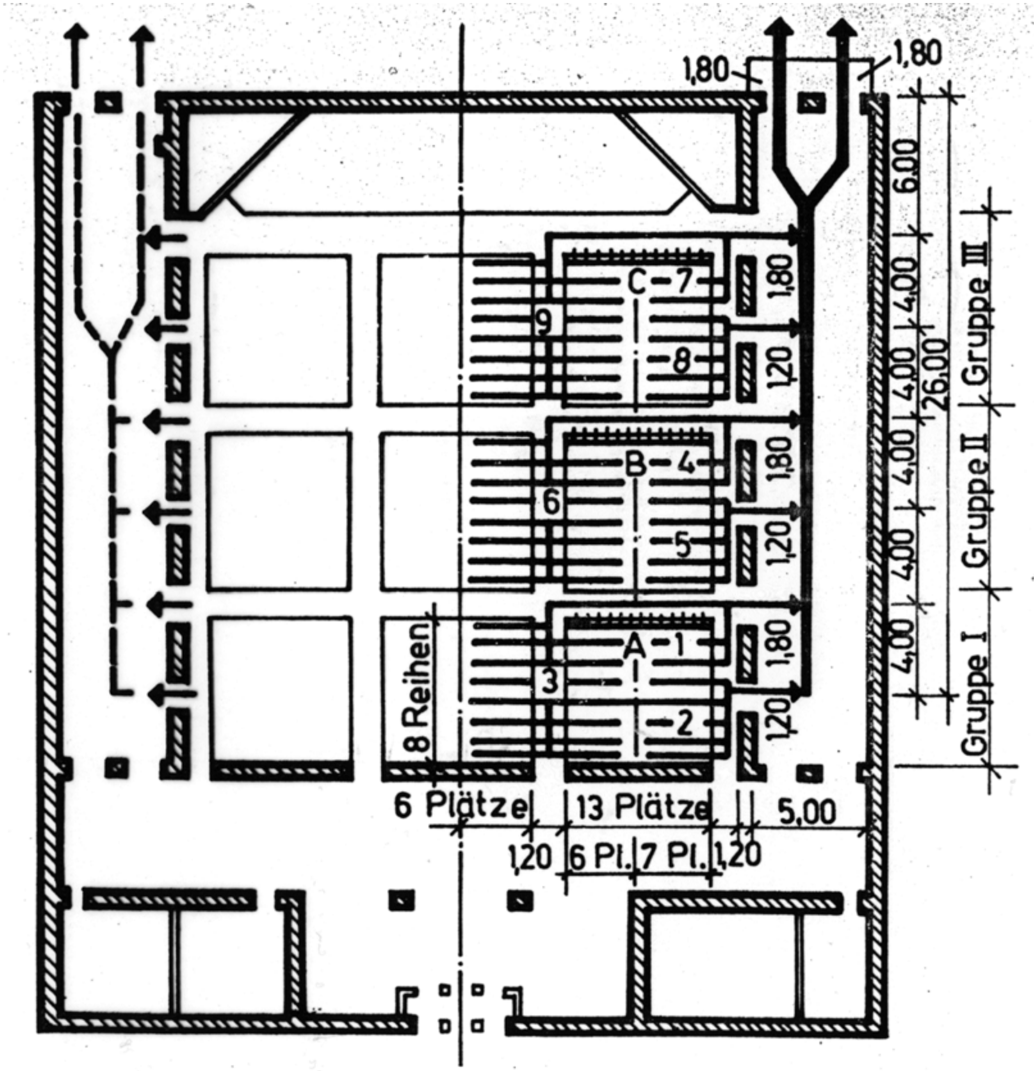

Abb. 92:
Schema der Personenevakuierung aus einem Kino

Lines of Equal Evacuation Times

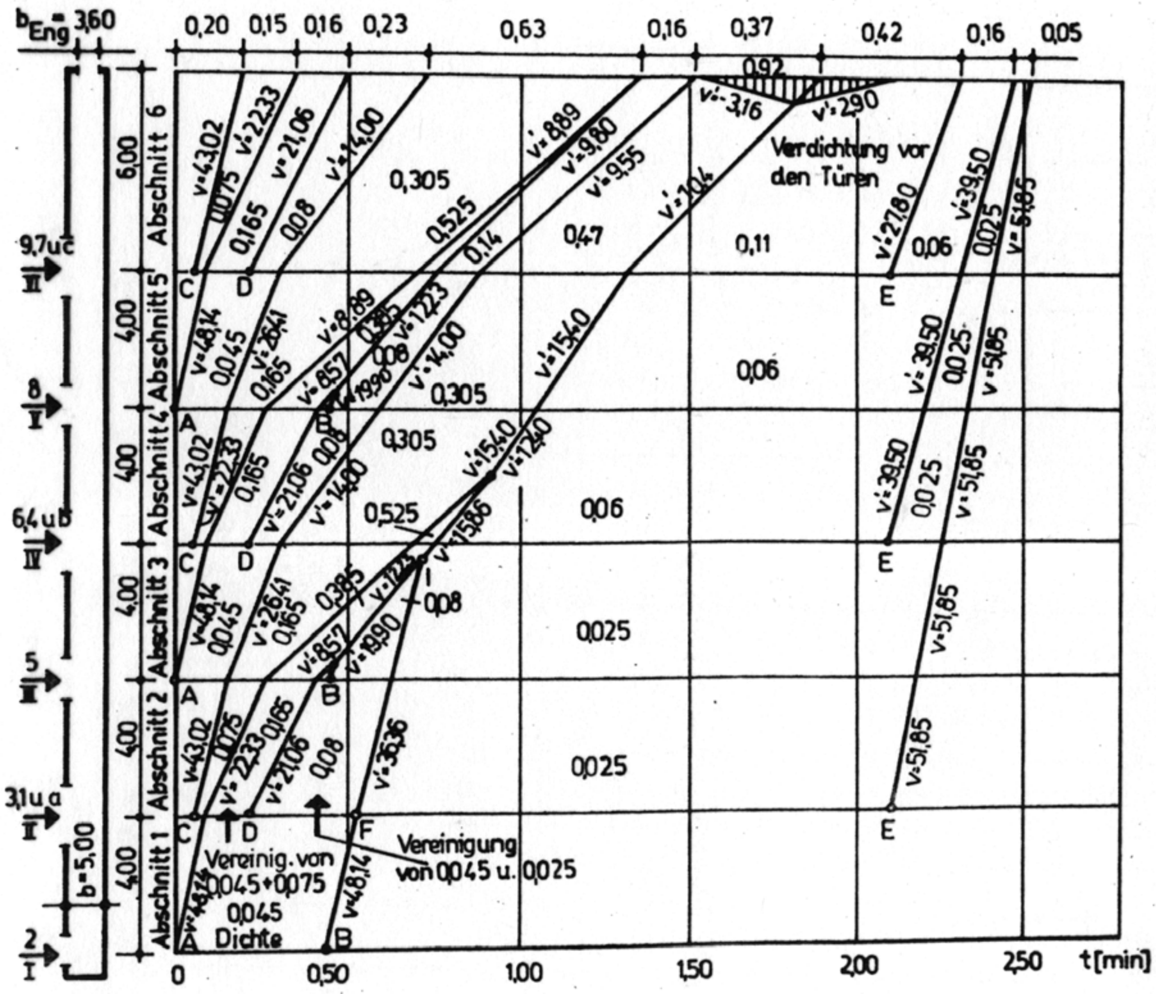

Abb. 94:
Grafische Darstellung der Bewegung vom Saal bis zum Ausgang aus dem Gebäude

Microsimulation of Crowd Dynamics

Simulation of the Sydney Olympic Park (Source: Keith Still)

Identification of Focal Routes and Conflict Points

Space utilization (Source: Keith Still)

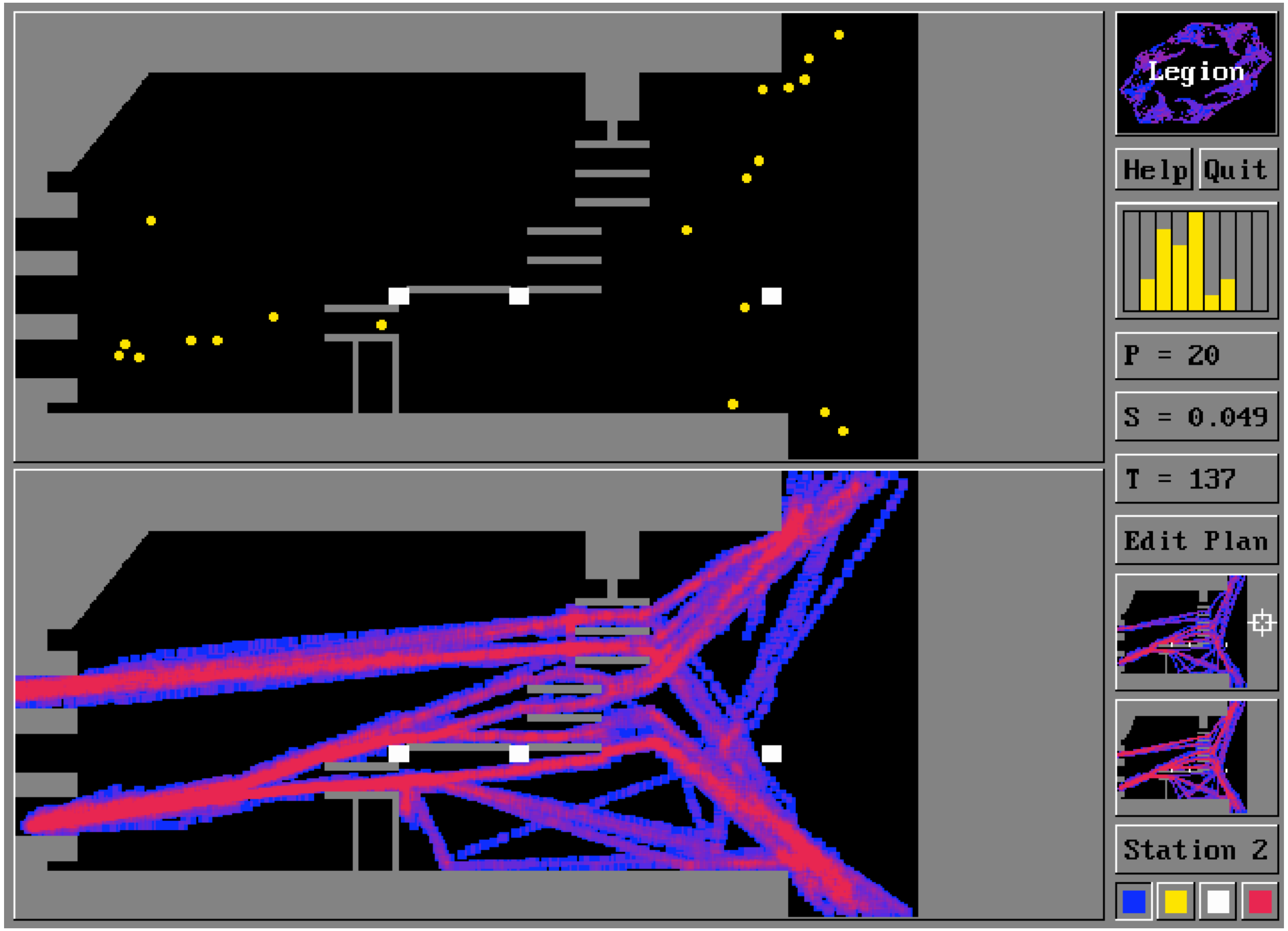

Identification of Bottlenecks

Bottlenecks at Kowloon-Canton Railway (Source: Keith Still)

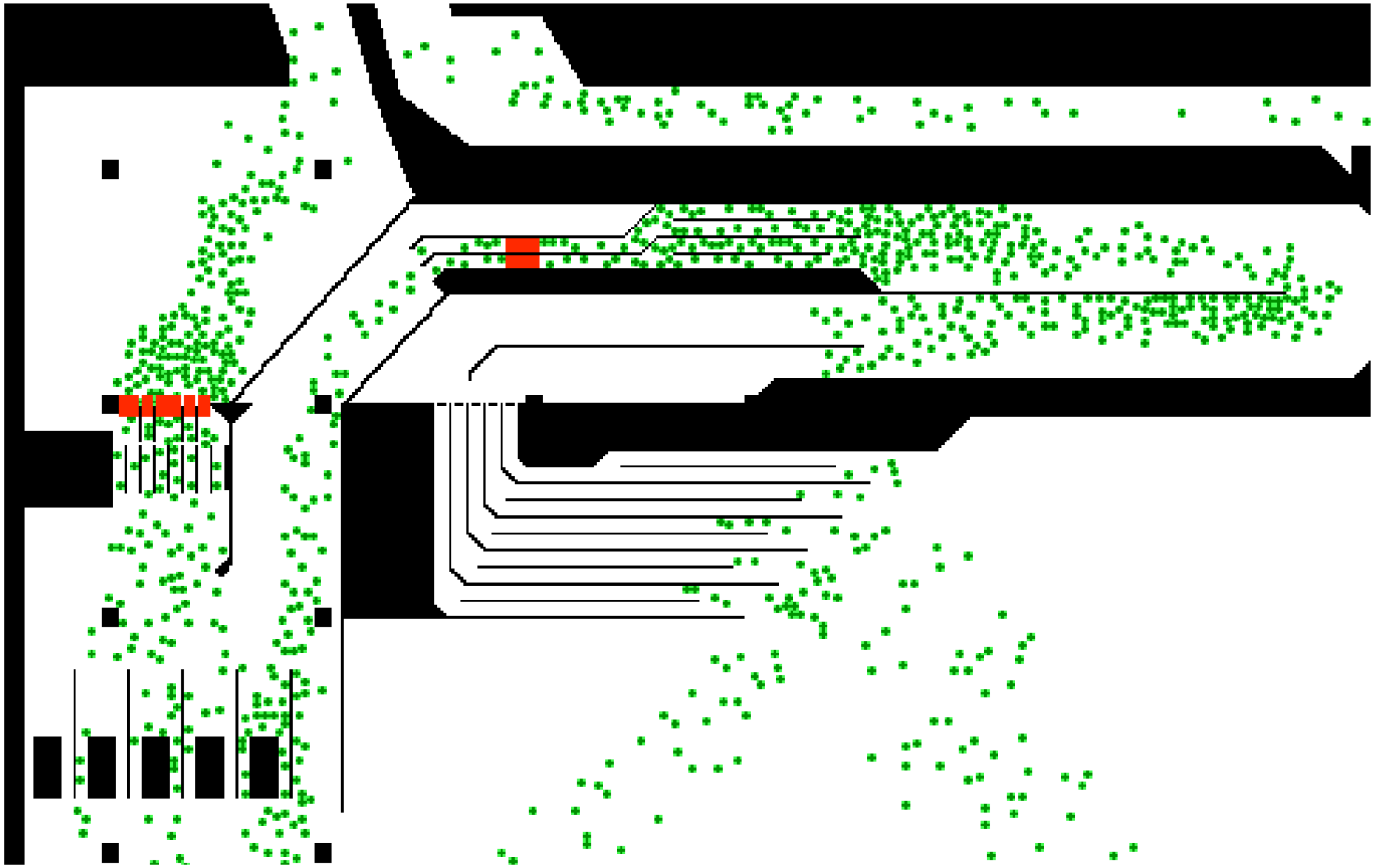

How Realistic are Today’s Evacuation Softwares?

- Today, many simulation software packages are available for the analysis of evacuation scenarios, e.g.
- VISSIM
- Arena
- Aseri
- EXODUS
- Legion
- Simulex
- TraffGo
- and others.
- Do these simulation programs describe real observations well? (Ask Armin Seyfried, Forschungszentrum Jülich)

Critical Evaluation of Models

- **LOS and Regression Models:** Suited for first drafts of layouts, but neglect dynamic interaction and self-organization effects
- **Cellular Automata Models:** Very fast, but neglect compressibility of and pressures in crowds; require artificial assumptions to produce realistic models; low predictive power
- **Still's model:** Even faster, but neglects direct pedestrian interactions, replaces them by some effective dynamics
- **Gas-kinetic models:** Take into account velocity distributions and densities, but high numerical effort
- **Fluid-dynamic models:** Efficient and suited for shock wave analysis, but neglect discrete, granular nature of crowd
- **Queuing models:** Suited for huge crowds with compartment structure, but neglect dynamics within the compartments
- **Social force model:** Realistic representation of interaction and self-organization effects and pressures in the crowd, but high numerical effort (supercomputers needed)

How to Construct a Realistic Model: The Social Force Concept

- Pedestrians are confronted with standard situations.
- The reactions to these are rather automatic.
- We assume a more ore less optimized behavior regarding the avoidance of collision and time delays.
- This allows us to describe the average behavior in a mathematical way.
- In addition, we have to consider fluctuations.
- We model the systematic contribution to the acceleration by a superposition of several (Non-Newtonian) forces reflecting different motivations and influence factors.
- The social force model offers a realistic representation of flexible space usage, interaction and self-organization effects as well as pressures in the crowd (at a relatively high numerical effort)

Emergence of Coordination in Pedestrian Counterflows

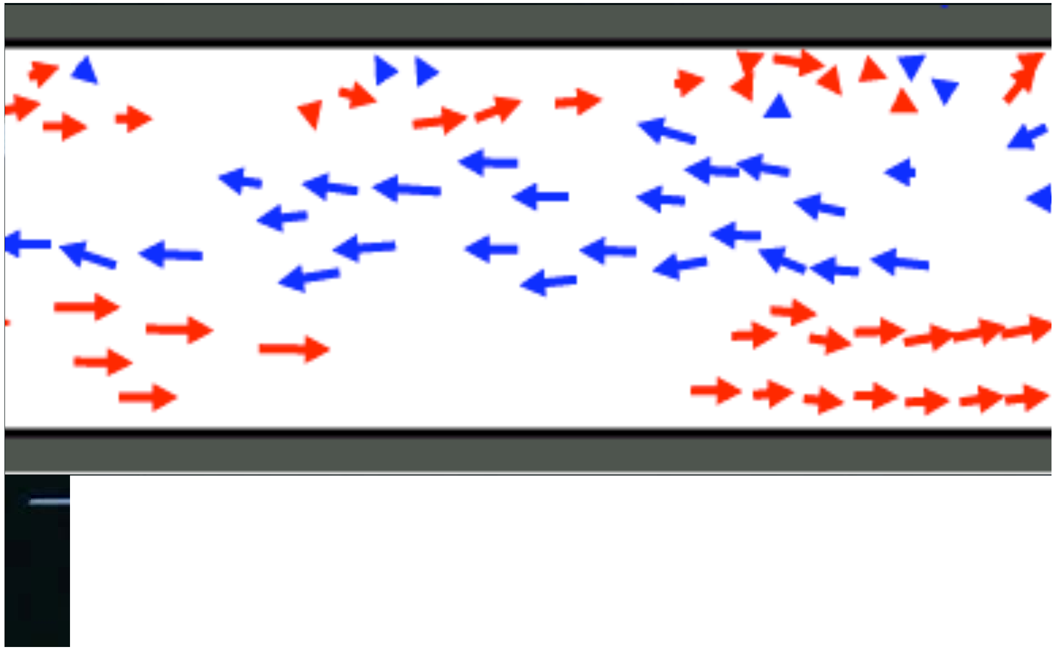

Based on individual interactions, lanes of uniform walking directions emerge in pedestrian crowds by self-organization. This constitutes a „macroscopic" social structure. Nobody orchestrates this collective behavior, and most people are not even aware of it.

Lane Formation in Pedestrian Counter Flows

Fluid-Induced Particle Size Segregation in Sheared Granular Media

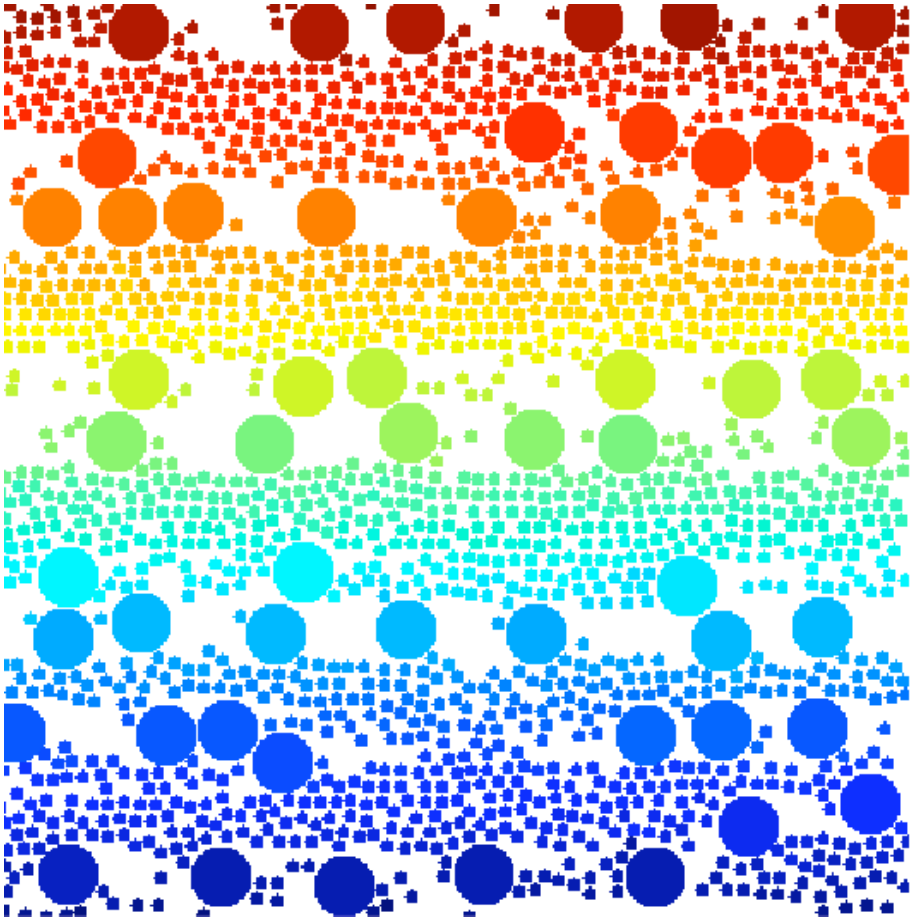

S. B. Santra, S. Schwarzer, and H. J. Herrmann, *Phys. Rev. E* **54**, 5066 (1996).

Role of Fluctuations

Small Fluctuations: Lane Formation

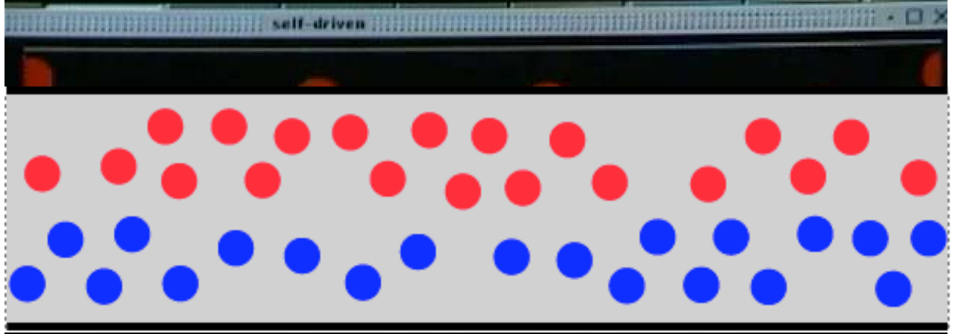

Large Fluctuations: "Freezing by Heating"

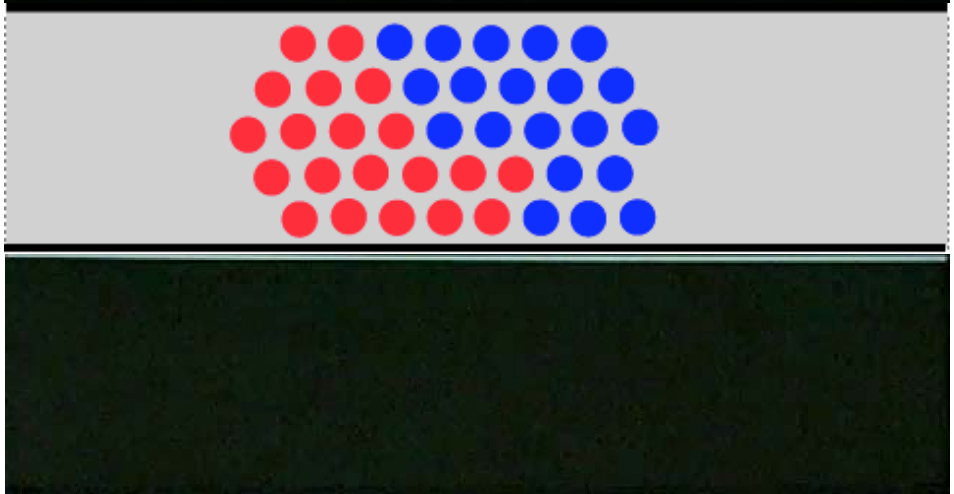

Ensemble-Averaged Efficiency

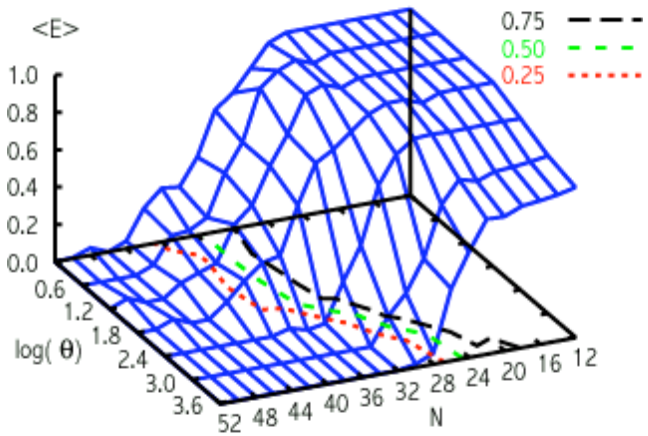

Reminder:
The temperature is proportional to the velocity variance.

D.H., I. Farkas, T. Viscek, *Phys. Rev. Lett.* **84**, 1240 (2000).

Experiments: Corridor with Bottlenecks

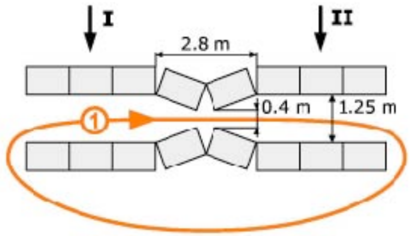

Experiment 1: Uni-directional pe-destrian streams passing a short bottleneck

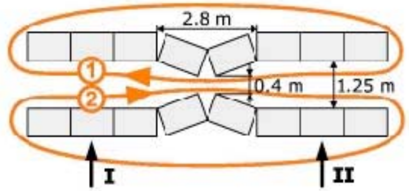

Experiment 2: Pedestrian counter-flows in a corridor with a short bottle-neck

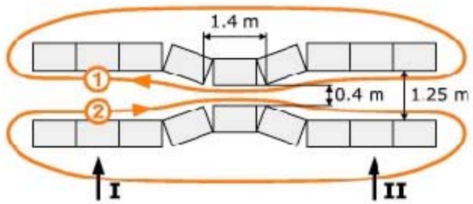

Experiment 3: Pedestrian counter-flow in a corridor with a long bottleneck

Bottlenecks

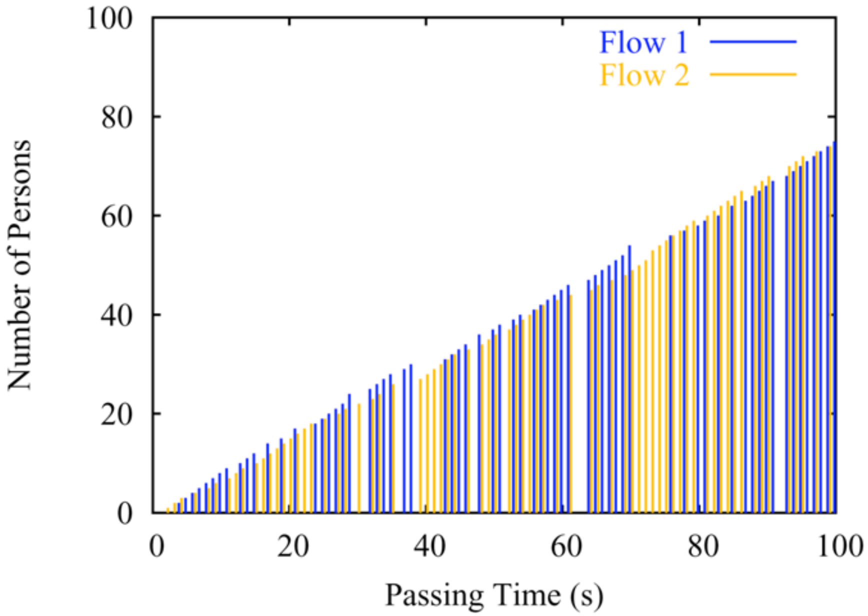

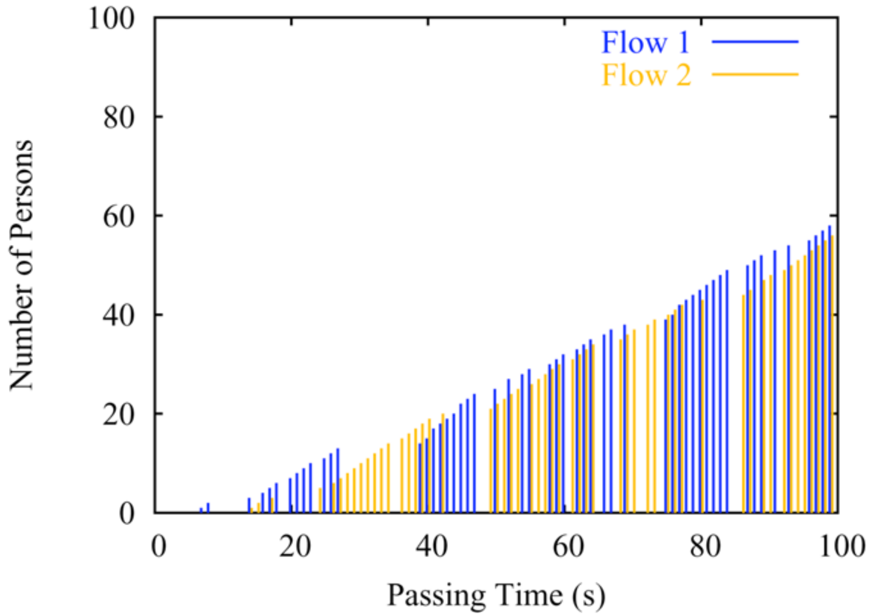

Compared to the flow through a corridor without narrowings the pedestrian flow after a short bottleneck is less regular due to oscillations in the passing direction. Pedestrians of the same direction of motion have a slight tendency to cluster (left).

At long bottlenecks, the oscillations in the passing direction are significantly more pronounced than at short bottlenecks. Moreover, the oscillation frequency is lower. There is a high tendency that the bottleneck is passed by clusters of pedestrians with the same direction of motion rather than by single individuals in an alternating manner (right).

Oscillatory Pedestrian Flows at Bottlenecks

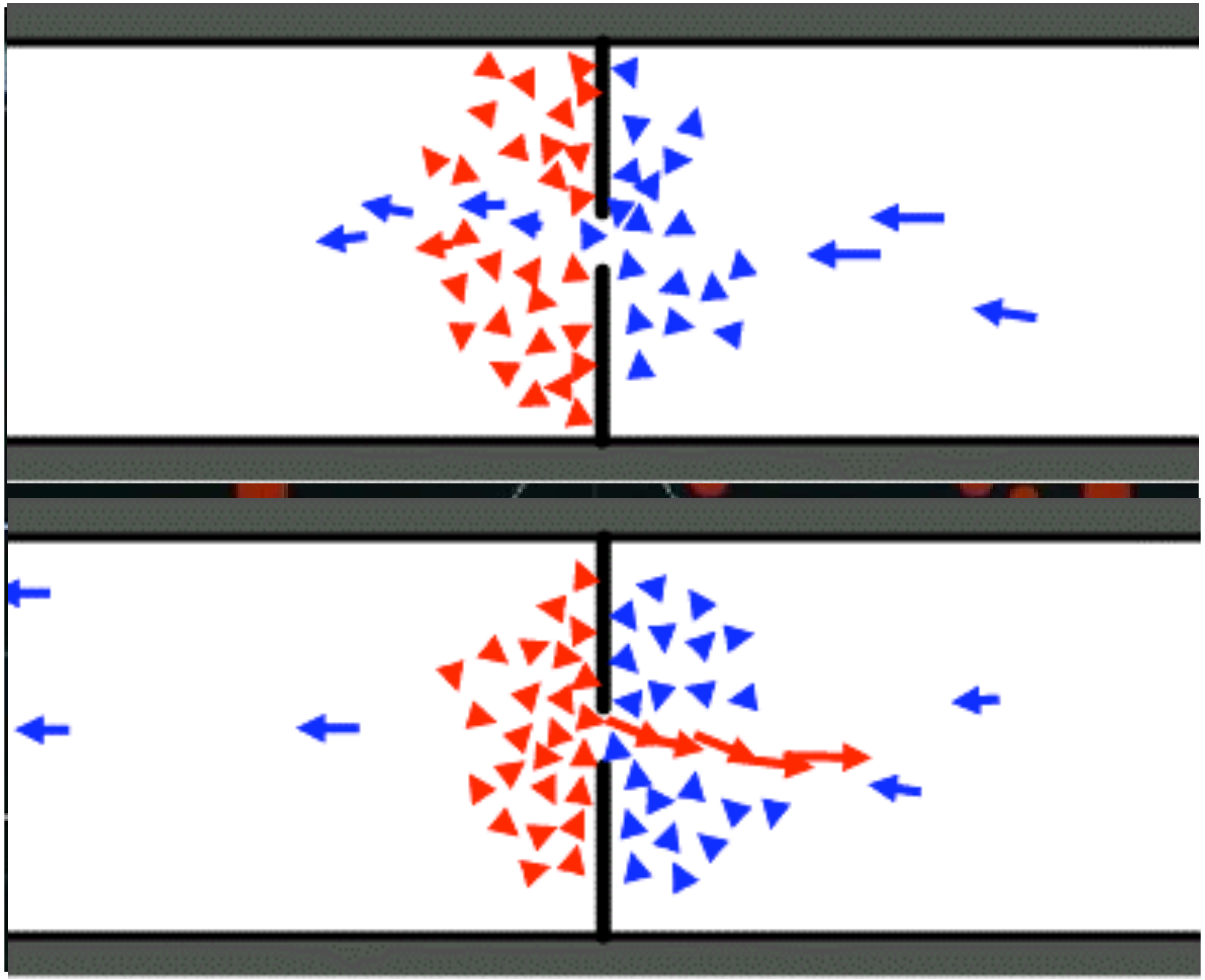

Experiments on Intersections and Widenings

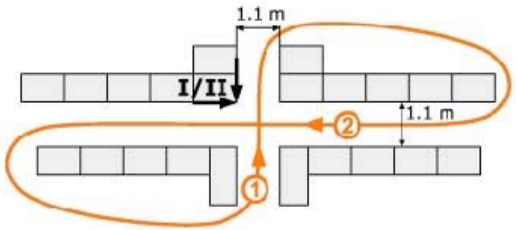

Experiment 4: Intersection of two perpendicular pedestrian streams

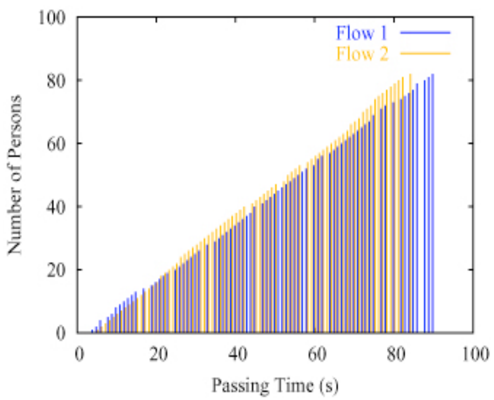

Experiment 5: Cross section of a corridor without narrowings

The Social Force Model

The social force model assumes individual goals (to reach a certain destination efficiently), social interactions (e.g. avoidance of collisions), and institutional setting (e.g. walls). It is composed of the following forces:

- Driving forces (to maintain the desired walking direction and speed)
- Social repulsive forces (to keep a private sphere around oneself)
- Social attractive forces among group members
- Repulsive forces reflecting the influence of walls
- Fluctuation forces describing variations in behavior

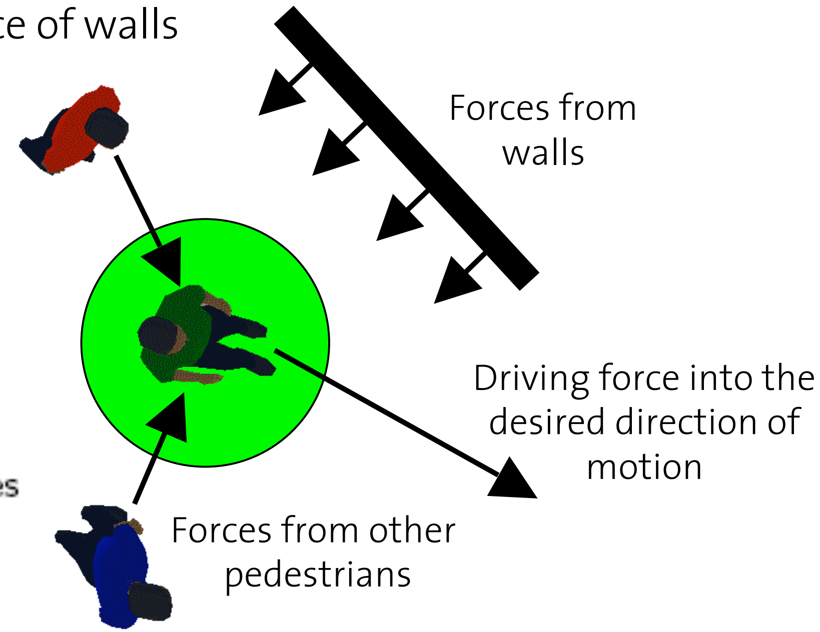

$$\frac{d\boldsymbol{x}_\alpha}{dt} = \boldsymbol{v}_\alpha(t) \quad \text{(equation of motion)}$$

$$\underbrace{\frac{d\boldsymbol{v}_\alpha}{dt}}_{\text{acceleration}} = \underbrace{\frac{1}{\tau_\alpha}(v_\alpha^0 \boldsymbol{e}_\alpha^0 - \boldsymbol{v}_\alpha)}_{\text{driving force}} + \underbrace{\sum_{\beta(\neq\alpha)} \boldsymbol{F}_{\alpha\beta}^{\text{int}}}_{\text{interactions}} + \underbrace{\boldsymbol{F}_\alpha^{\text{walls}}}_{\text{boundaries}}$$

(acceleration equation)

As people show a pretty standard behavior in walking interactions and constrain each others' motion, the dynamics of crowds can be relatively well predicted.

The Social Forces Framework: A Successful Approach

- Driving Force
- Repulsive Force
- Wall Repulsion
- Effective acceleration

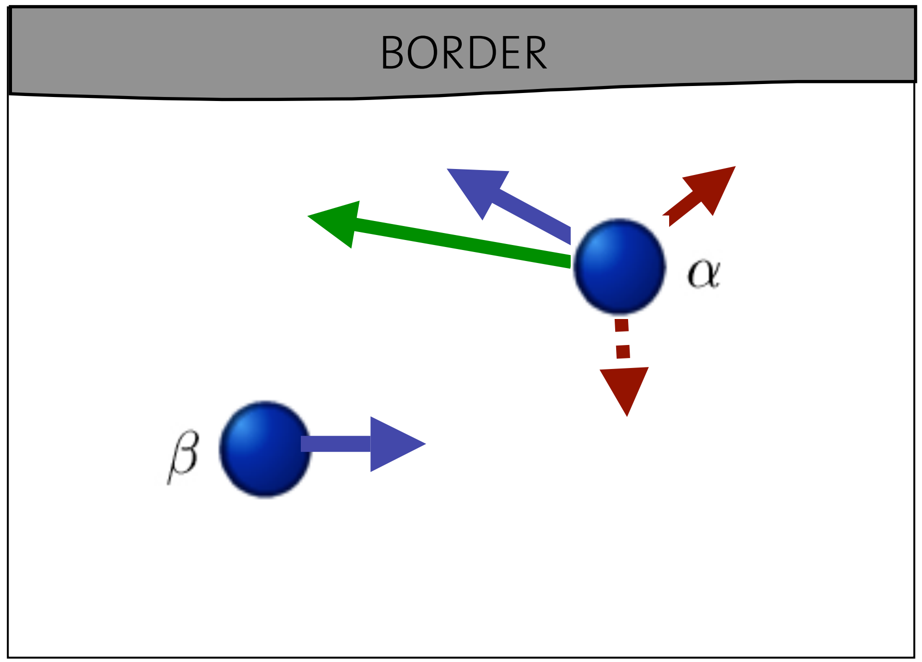

$$F_{obs}(t) = F_d(t) + F_{walls}(t) + F(t)$$

Behavior in Conflict Situations and Superposition of Forces

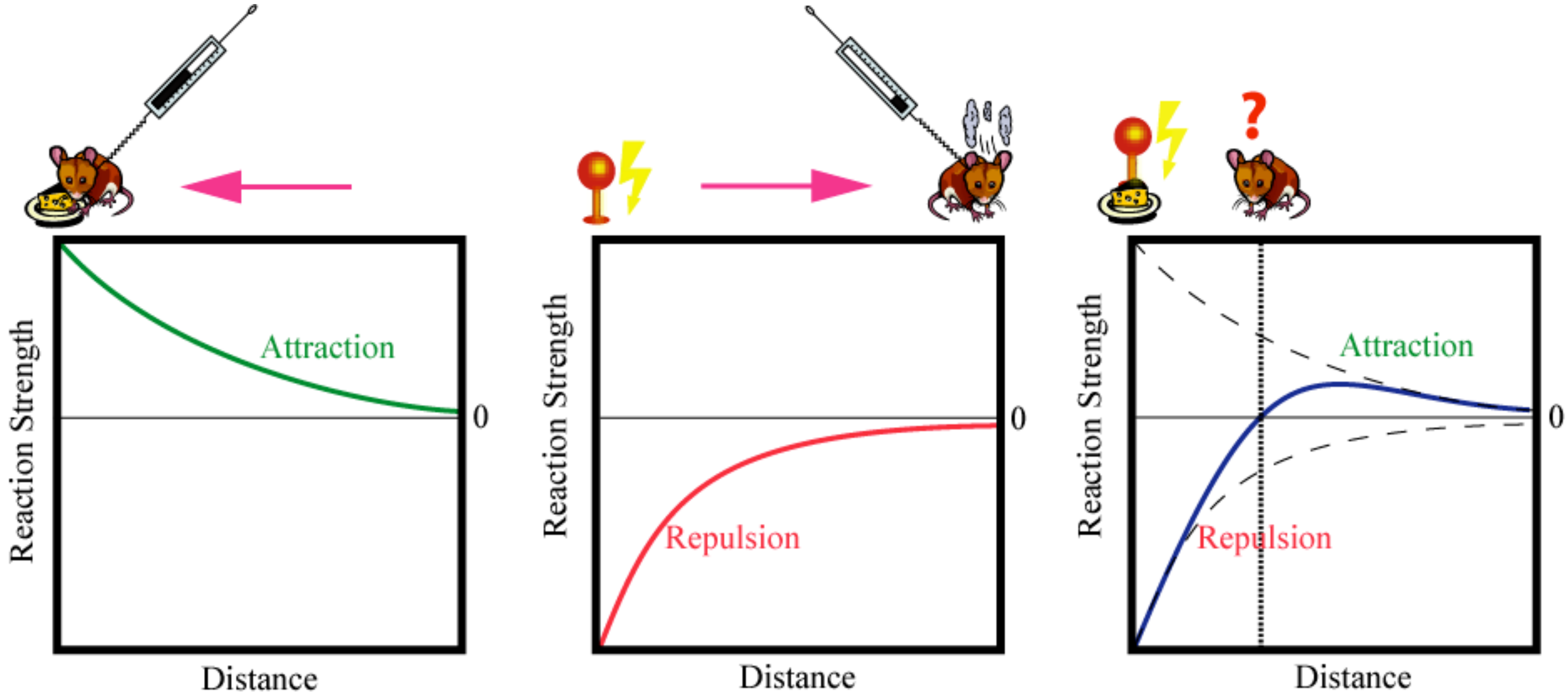

Social Force Model of Pedestrian Dynamics

Equation of Motion:

$$\frac{d\vec{x}_i(t)}{dt} = \vec{v}_i(t)$$

Acceleration Equation for Pedestrians:

$$\underbrace{m_i \frac{d\vec{v}_i(t)}{dt}}_{\text{Acceleration}} = \underbrace{\frac{m_i}{\tau_i}\left(v_i^0 \vec{e}_i(t) - \vec{v}_i(t)\right)}_{\text{Driving Force}} + \underbrace{\sum_{j(\neq i)} \vec{F}_{ij}^{ww}(t)}_{\text{Interactions}} + \underbrace{\vec{F}_i^{b}(t)}_{\text{Borders, Fire}} + \underbrace{\sum_{k} F_{ik}^{att}(t)}_{\text{Attractions}} + \underbrace{\vec{\xi}_i(t)}_{\text{Fluctuations}}$$

$$\vec{F}_{ij}^{ww}(t) = \underbrace{\vec{F}_{ij}^{psy}(t)}_{\text{Psychological Repulsion}} + \underbrace{\vec{F}_{ij}^{ph}(t)}_{\text{Physical Interactions}} + \underbrace{\vec{F}_{ij}^{att}(t)}_{\text{Attractions between People}}$$

$\vec{x}_i$ = Place; t = Time; $\vec{v}_i$ = Speed; m_i = Mass; $\hat{o}_i$ = Acceleration Time; v_i^0 = Desired Velocity;
$\vec{e}_i$ = Desired Direction

Evaluation of Pedestrian Trajectories

Calculate trend matrices:

$Trend_0 = Frame_n - Frame_{n-1}$

$Trend_1 = Frame_{n-1} - Frame_{n-2}$

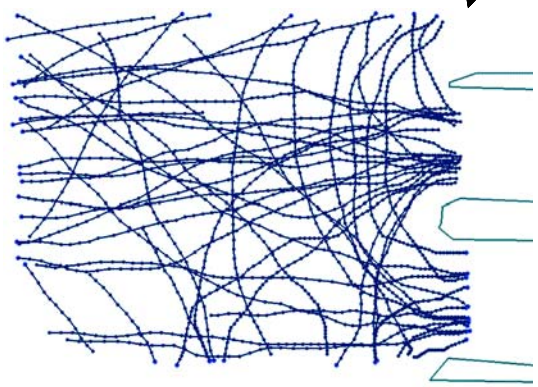

Recognize movement by searching for similarities in the local neighborhoods around each point in the trend matrices.

Transform the trajectory coordinates into the ground plane, by approximating each human to be 170 cm high.

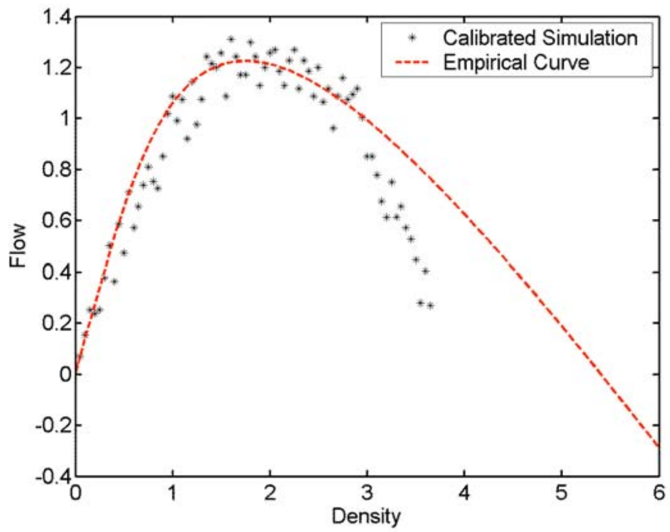

Elliptical Social Force Model

An improved, elliptical, specification of the social force model has been proposed, taking into account velocity and relative velocities. Δt reflects the time for a stride and b is the semi-minor axis of an ellipse directed into the direction of motion:

Repulsive potential:

$$V_{\alpha\beta}(b) = AB\,\mathrm{e}^{-b_{\alpha\beta}/B}$$

Repulsive force:

$$\vec{g}_{\alpha\beta}(\vec{d}_{\alpha\beta}) = -\vec{\nabla}_{\vec{d}_{\alpha\beta}} V_{\alpha\beta}(b_{\alpha\beta})$$

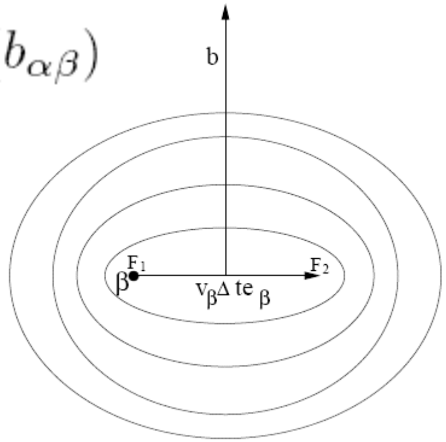

Elliptical specification I:

$$2b = \sqrt{(\|\vec{d}_{\alpha\beta}\| + \|\vec{d}_{\alpha\beta} - v_\beta\,\Delta t\,\vec{e}_\beta\|)^2 - (v_\beta\,\Delta t)^2}$$

Elliptical specification II:

$$2b = \sqrt{(\|\vec{d}_{\alpha\beta}\| + \|\vec{d}_{\alpha\beta} - (\vec{v}_\beta - \vec{v}_\alpha)\Delta t\|)^2 - [(\vec{v}_\beta - \vec{v}_\alpha)\Delta t]^2}$$

Calibration with Genetic Algorithms

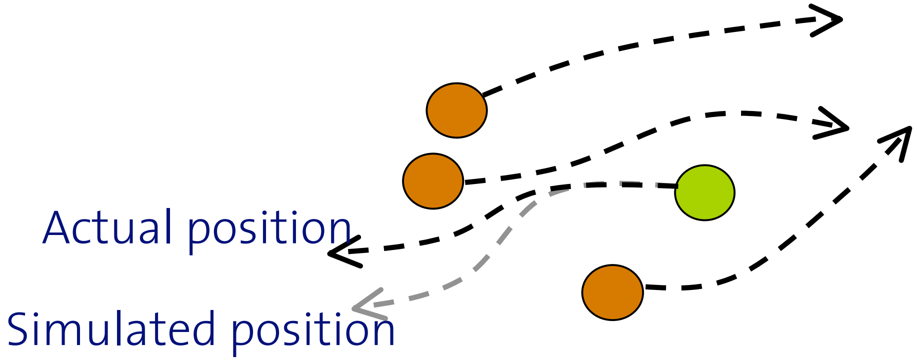

We use a hybrid model where n-1 of the n pedestrians are moving according to the trajectories from the videos, and 1 pedestrian is controlled by a micro-simulation. Then we have an error measure related to the deviation from our simulated position and the actual position from the video. With this error measure we can iterate a calibration process that will find an optimal set of simulation parameters.

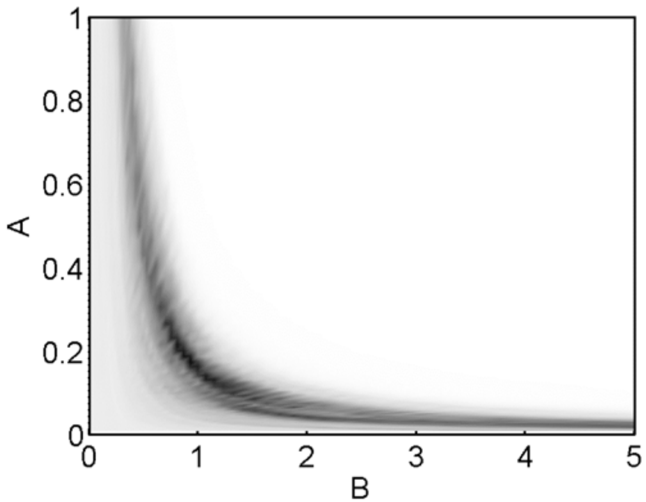

Model	A	B	λ	Fitness
Circular	0.11 ± 0.06	0.84 ± 0.63	1	-0.65
Elliptical I	1.52 ± 1.65	0.21 ± 0.08	1	-0.67
Elliptical II	4.30 ± 3.91	1.07 ± 1.35	1	-0.47
Circular	0.42 ± 0.26	1.65 ± 1.01	0.12 ± 0.07	-0.60
Elliptical I	0.11 ± 0.01	1.19 ± 0.45	0.16 ± 0.04	-0.59
Elliptical II	0.04 ± 0.01	3.22 ± 0.67	0.06 ± 0.04	-0.39

Distance Dependence

The distance-dependent function is investigated at the distances, 0m, 0.5m, 1m, ..., 4.5m, and when fitting these values with the videos (black curve) it matches very well to an exponential function (blue dotted curve).

Black curve obtained from videos

Blue curve: exp(-d/0.5)

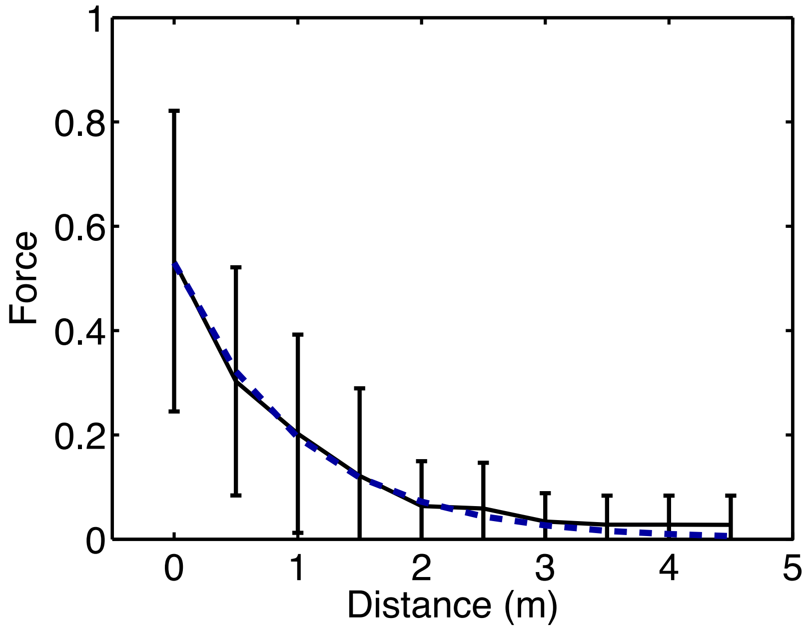

Angular Dependence

Similarly to how the distance-dependent function was obtained, we fit a polygon with 32 points distributed around each pedestrian, at fixed angles. When calibrating to the videos, it turns out that the angular dependence can be approximated with a half circle around the pedestrian.

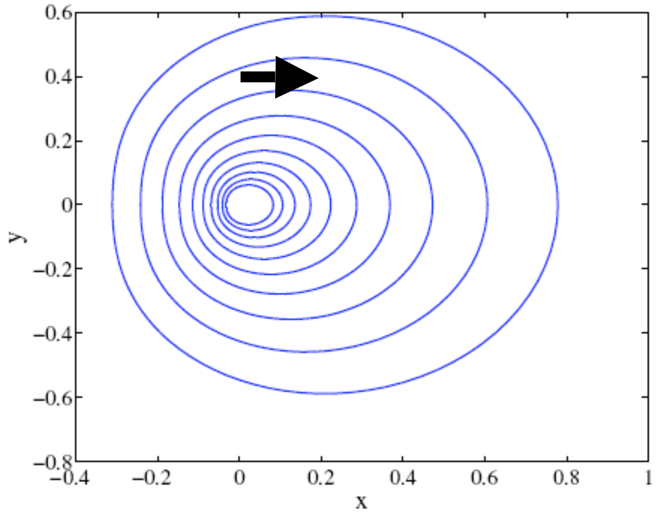

$$w(\varphi_{\alpha\beta}(t)) = \left(\lambda_\alpha + (1-\lambda_\alpha)\frac{1+\cos(\varphi_{\alpha\beta})}{2}\right)$$

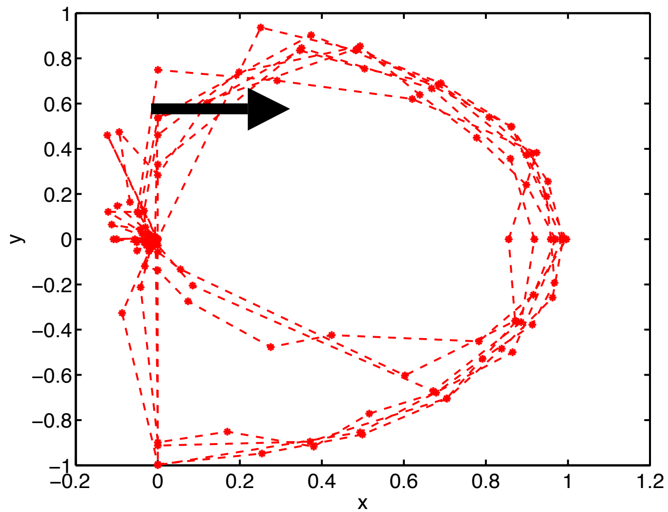

Polygons obtained from videos

Experimental Approach

- Individual Behavior
- Collective Dynamics

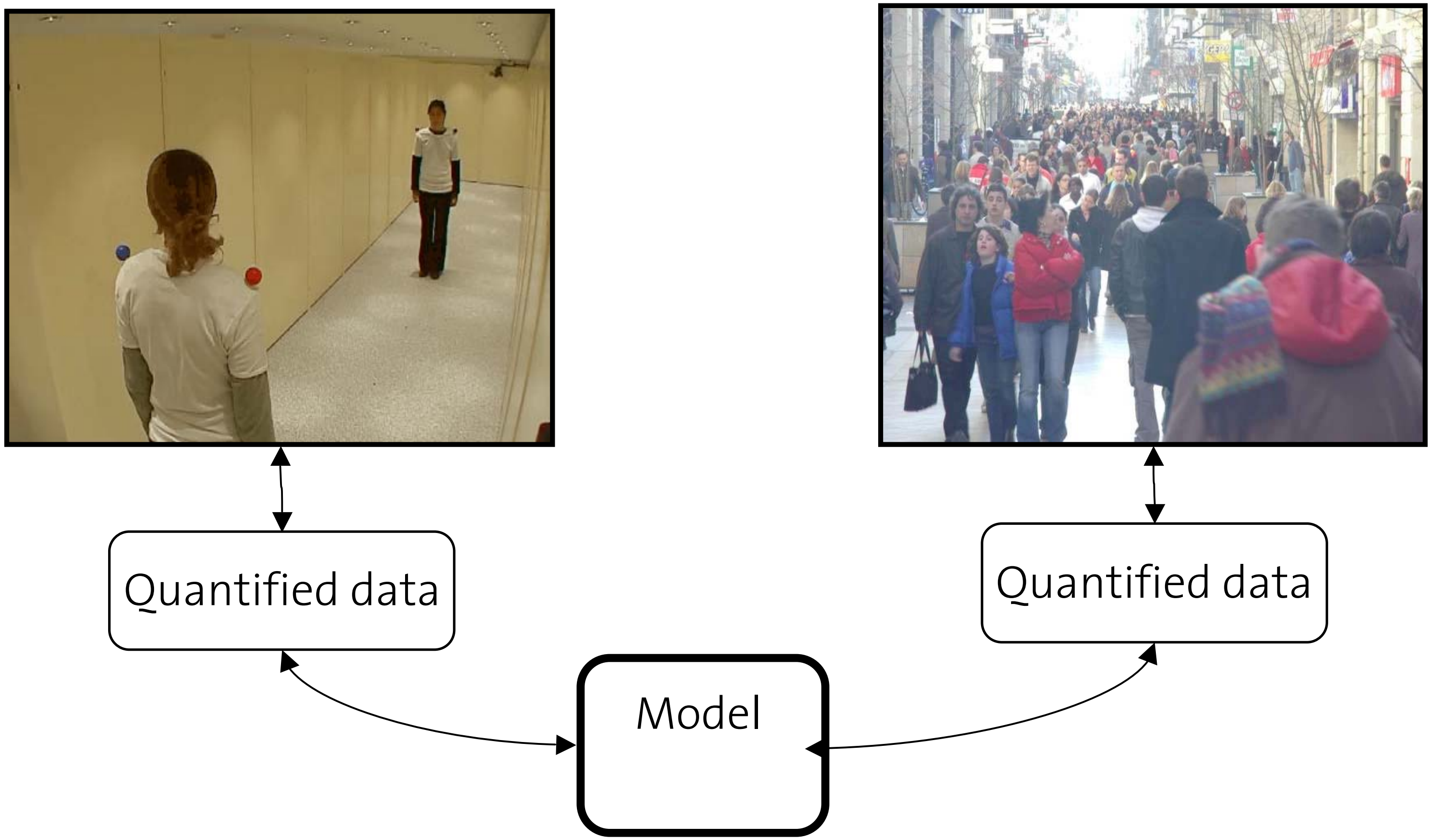

Individual Behavior

Setup 1

Single pedestrian's behavior

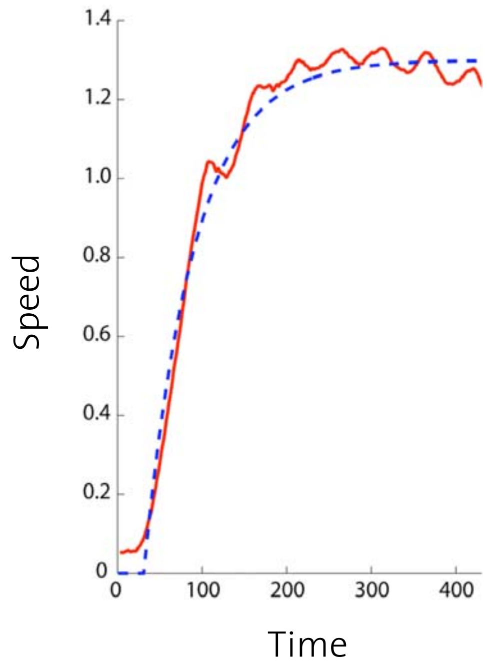

Average walking speed of single pedestrians

Individual Behavior

Setups 2 & 3

Avoidance of a static pedestrian

Avoidance of a moving pedestrian

Controlled Pedestrian Experiments

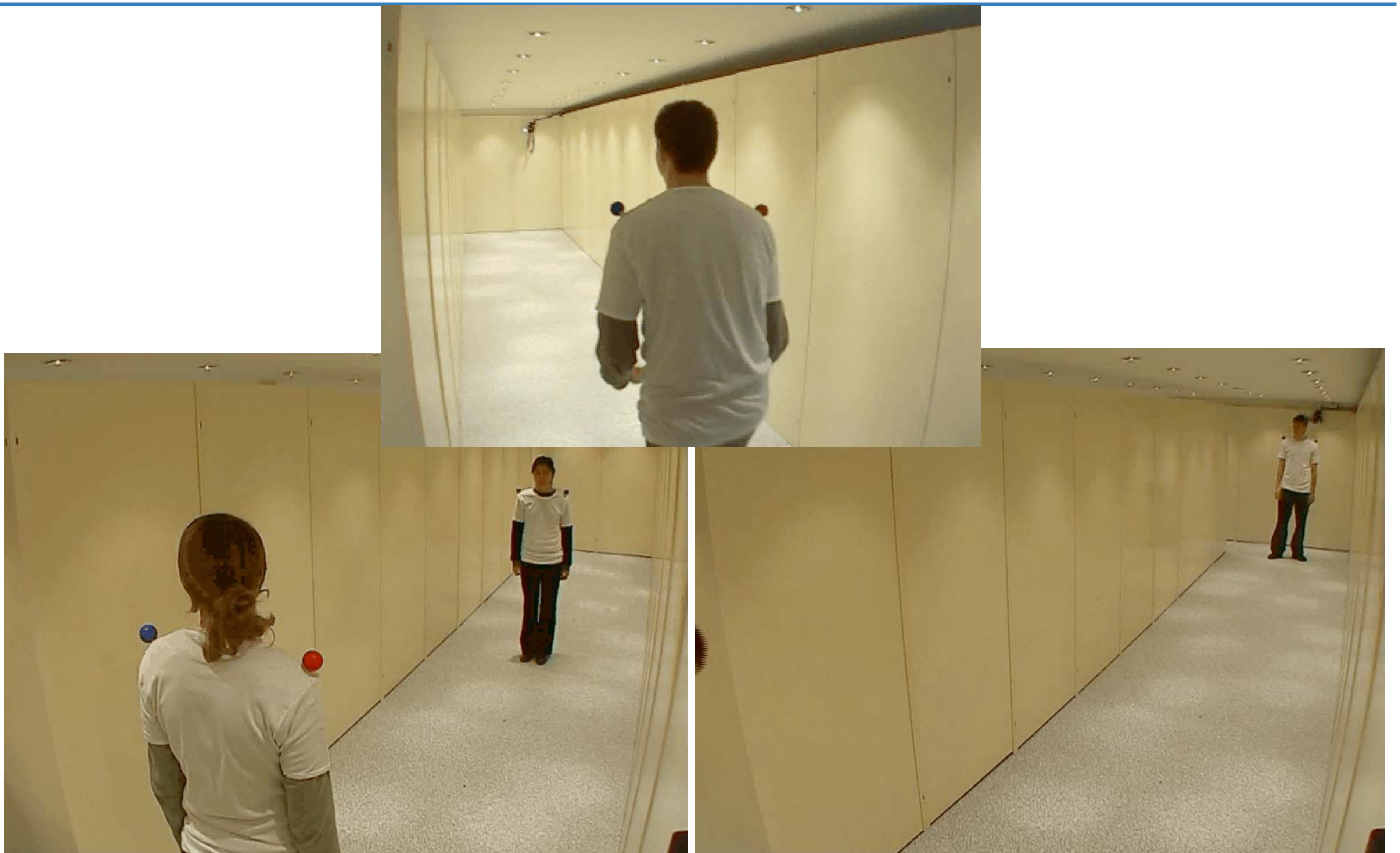

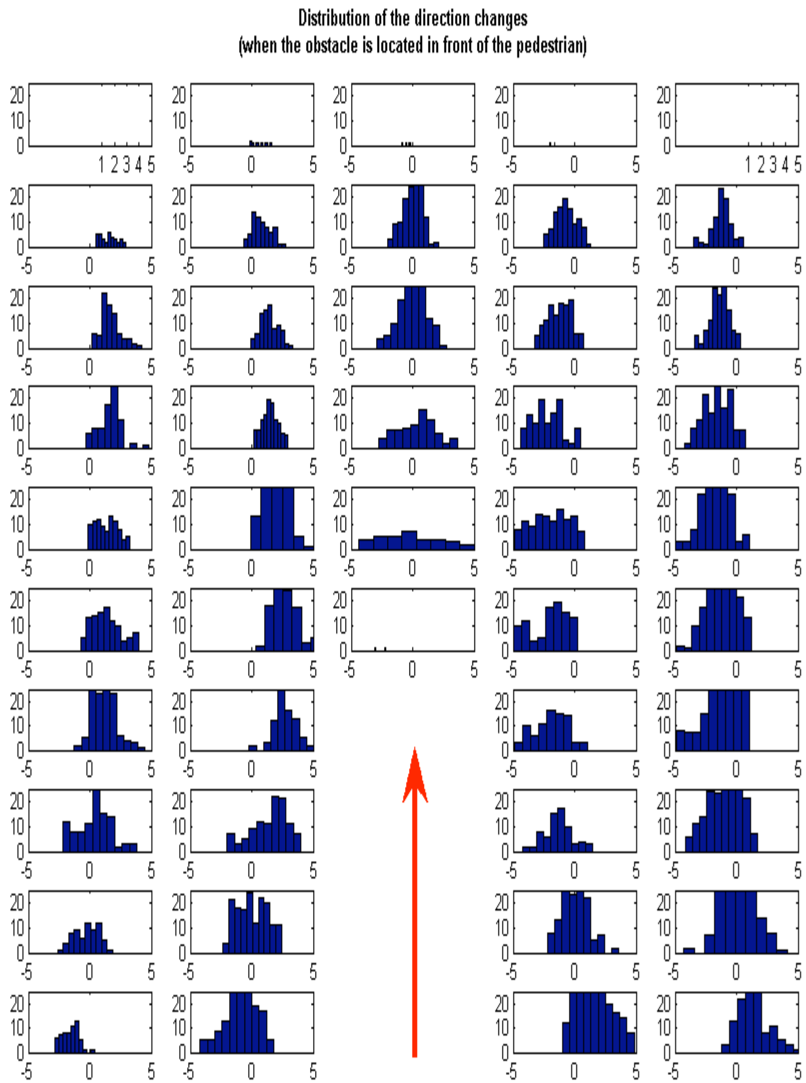
Distribution of the direction changes
(when the obstacle is located in front of the pedestrian)

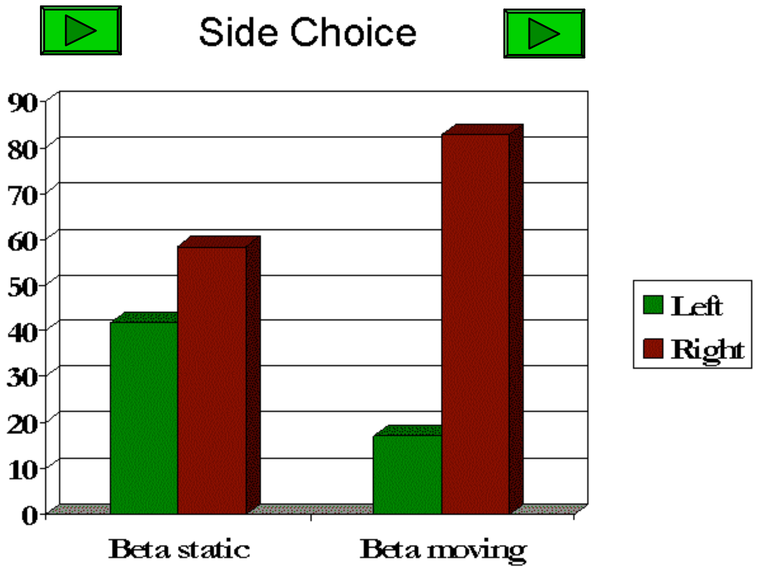
Side Choice
Beta static
Beta moving
Left
Right

Experiments on Human Interactions in Space

Work in progress
with Guy Theraulaz
and Mehdi Moussaid

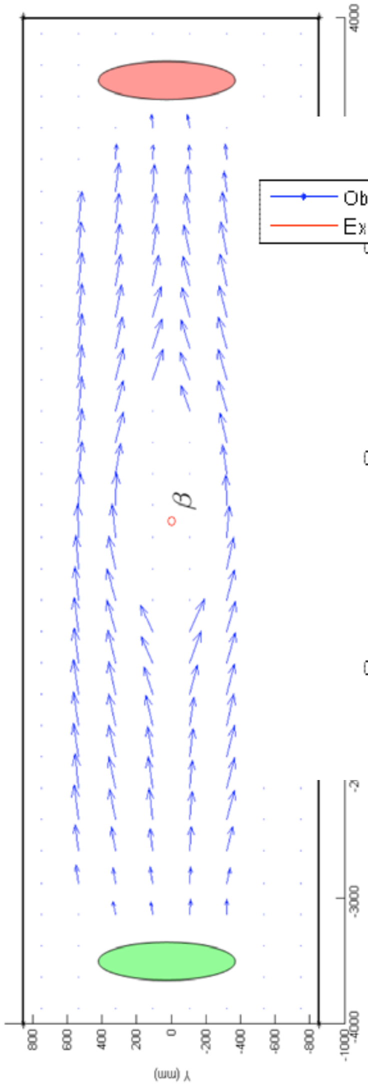

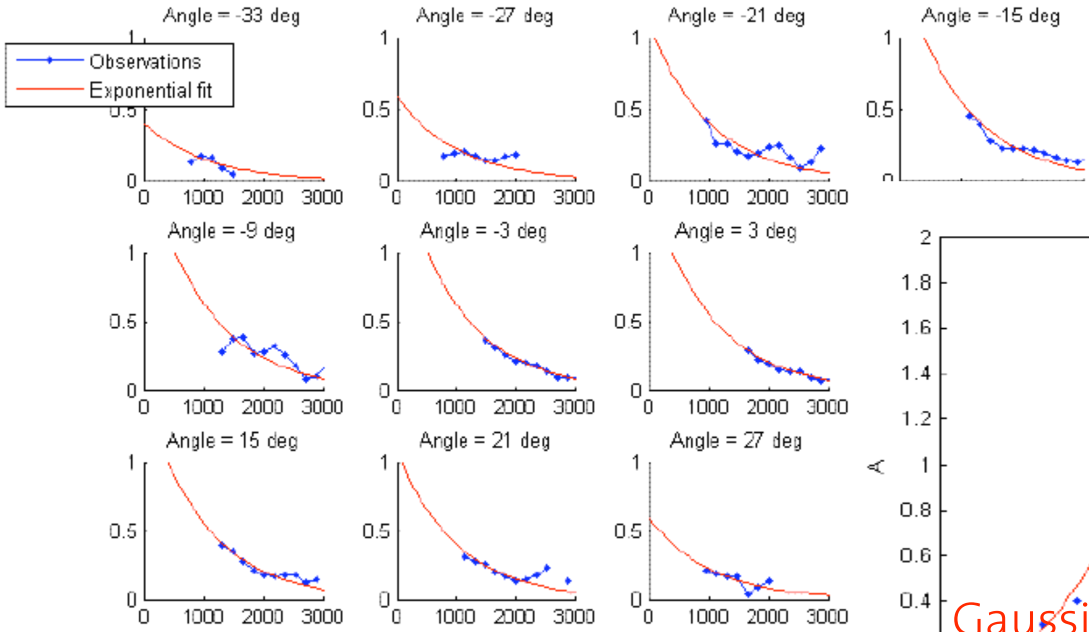

Exponential distance dependence

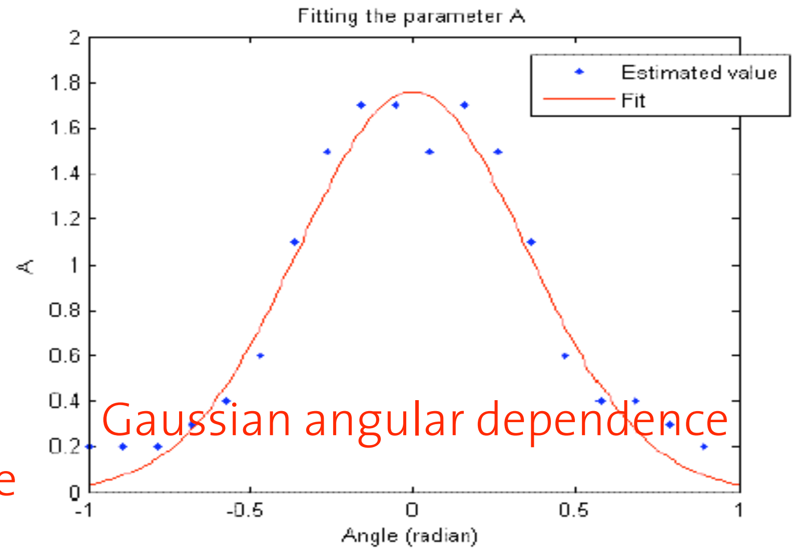

Gaussian angular dependence

$$F_{\alpha\beta}^{\text{int}} = \underbrace{F_v(d_{\alpha\beta},\varphi_{\alpha\beta})e_\alpha(t)}_{\text{velocity changes}} + \underbrace{[F_\varphi(d_{\alpha\beta},\varphi_{\alpha\beta})\xi_\alpha(\varphi_{\alpha\beta})]n_\alpha(t)}_{\text{directional changes}}$$

$$F_v(d,\varphi) = \mathrm{e}^{-5\varphi^2}\mathrm{e}^{-d} \qquad F_\varphi(d,\varphi) = 1.76\mathrm{e}^{-2\varphi^2}\mathrm{e}^{-d}$$

Side Choice Dynamics

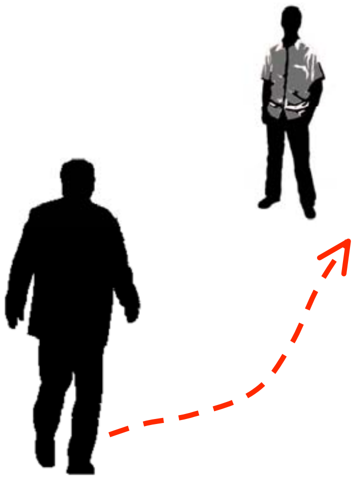

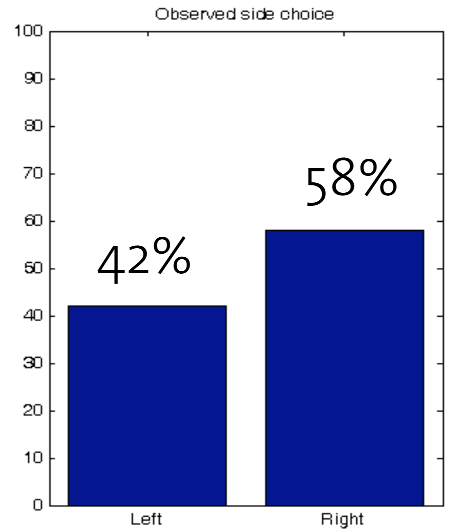

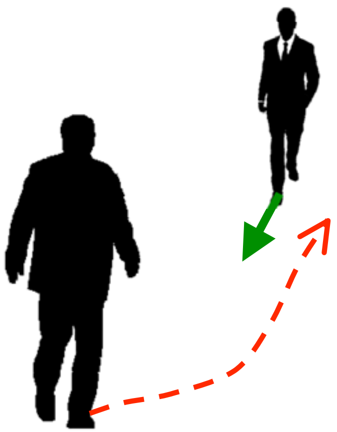

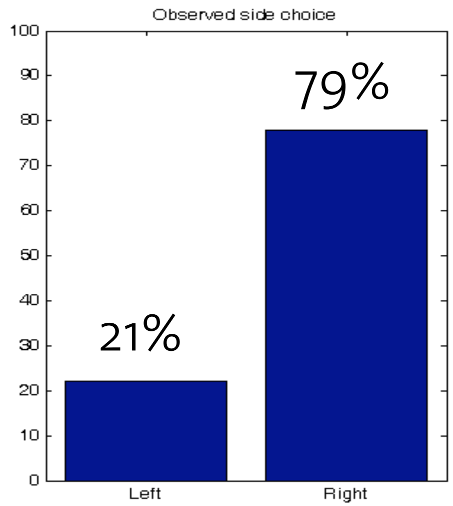

The Force Field - Data Representation

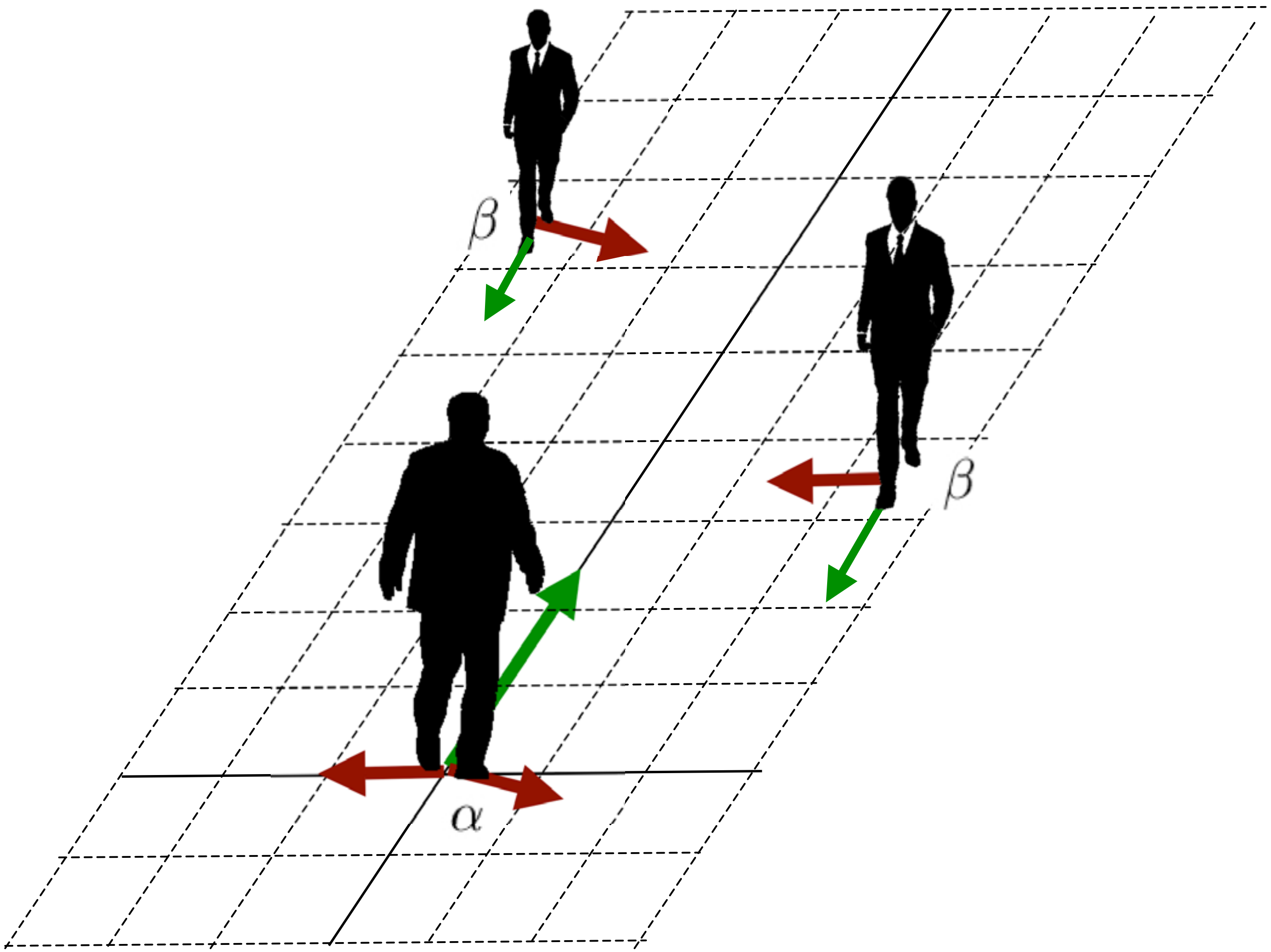

Empirical Force Field

- Repulsive field in front of a pedestrian
  - Sides area : Simple avoidance
  - Front area : Speed decrease

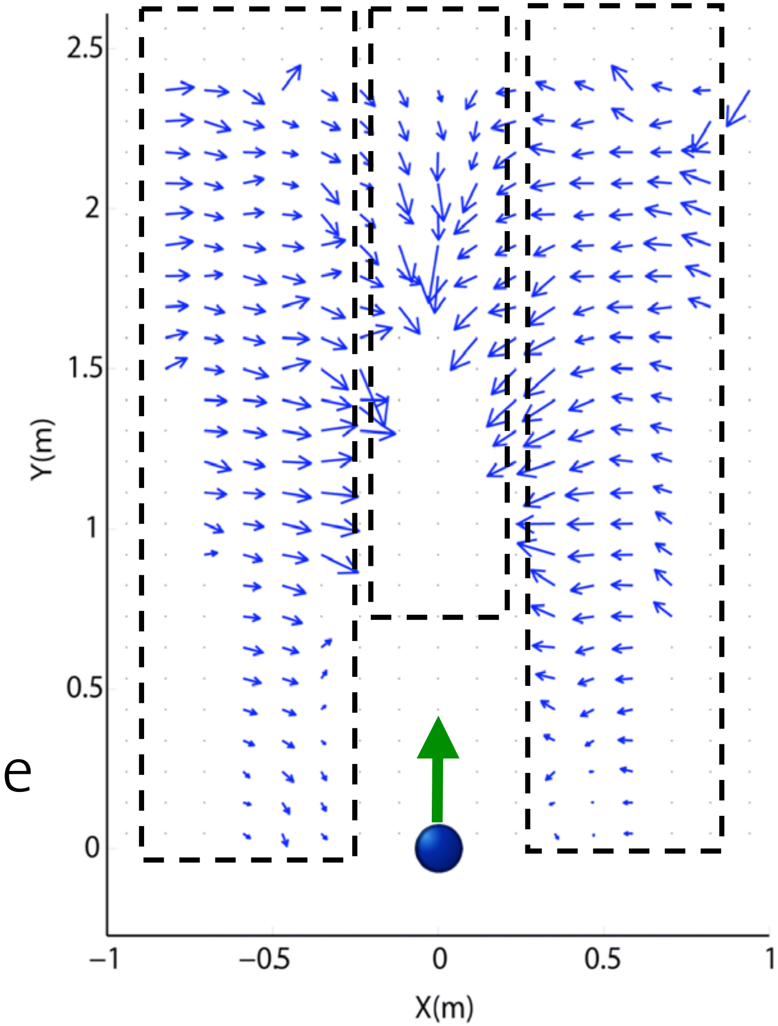

Fitting of the Force Field

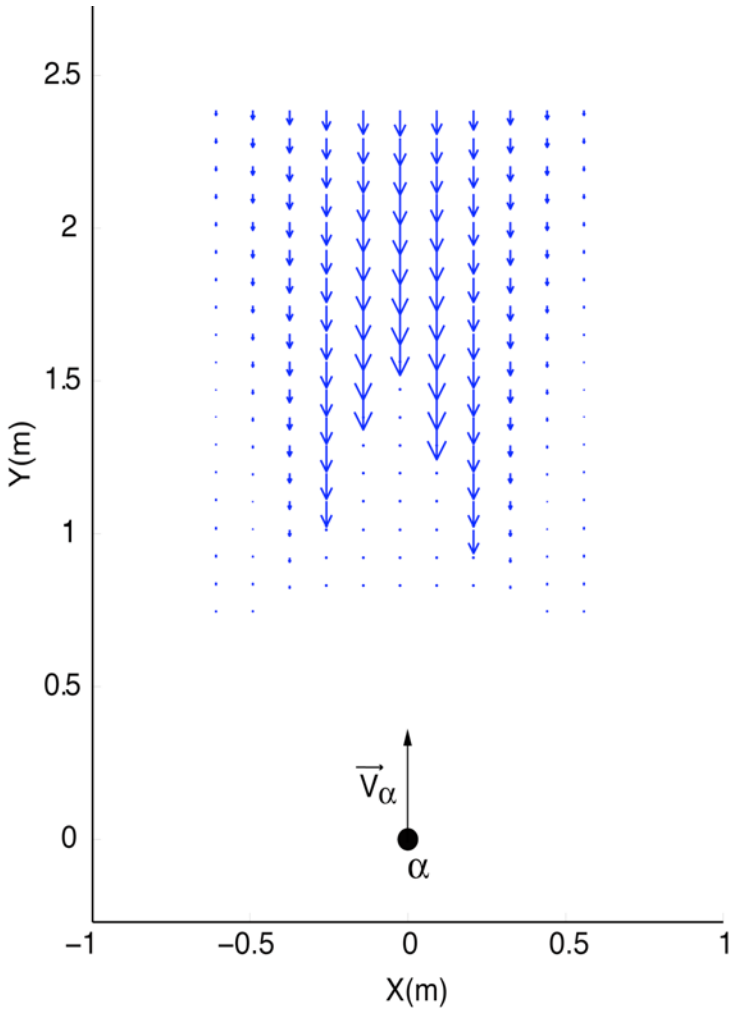

Speed Decease

Layer 2: Speed decrease

$$f_v(r,\theta) = -Ae^{-\frac{r}{B}-(n'B\theta)^2}$$

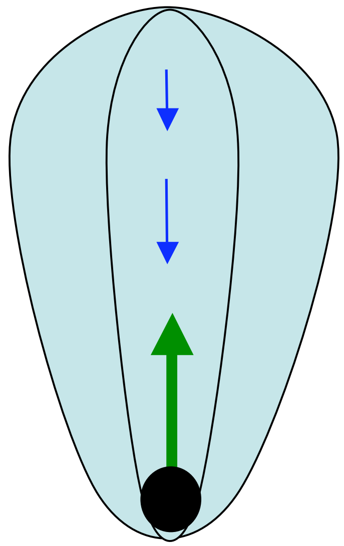

Fitting of the Force Field

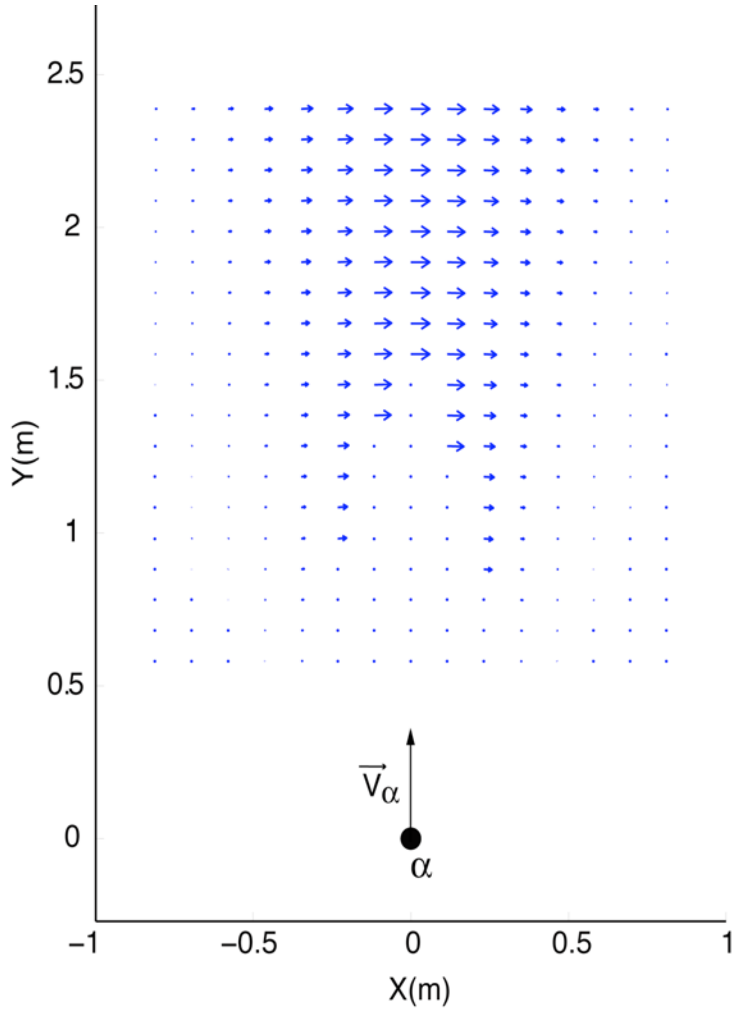

Side Preference

Layer 3: Side preference

$$f_h(\theta) = S||\overrightarrow{D}||e^{-(n'B\theta)^2}$$

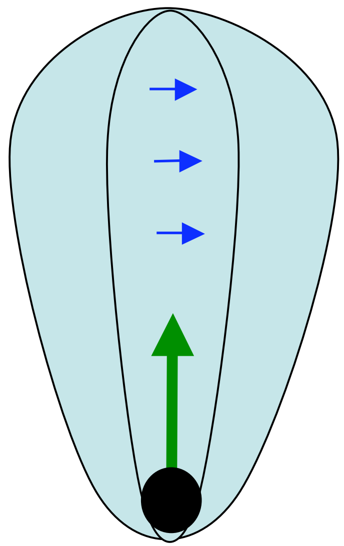

Comparison of Data and Model

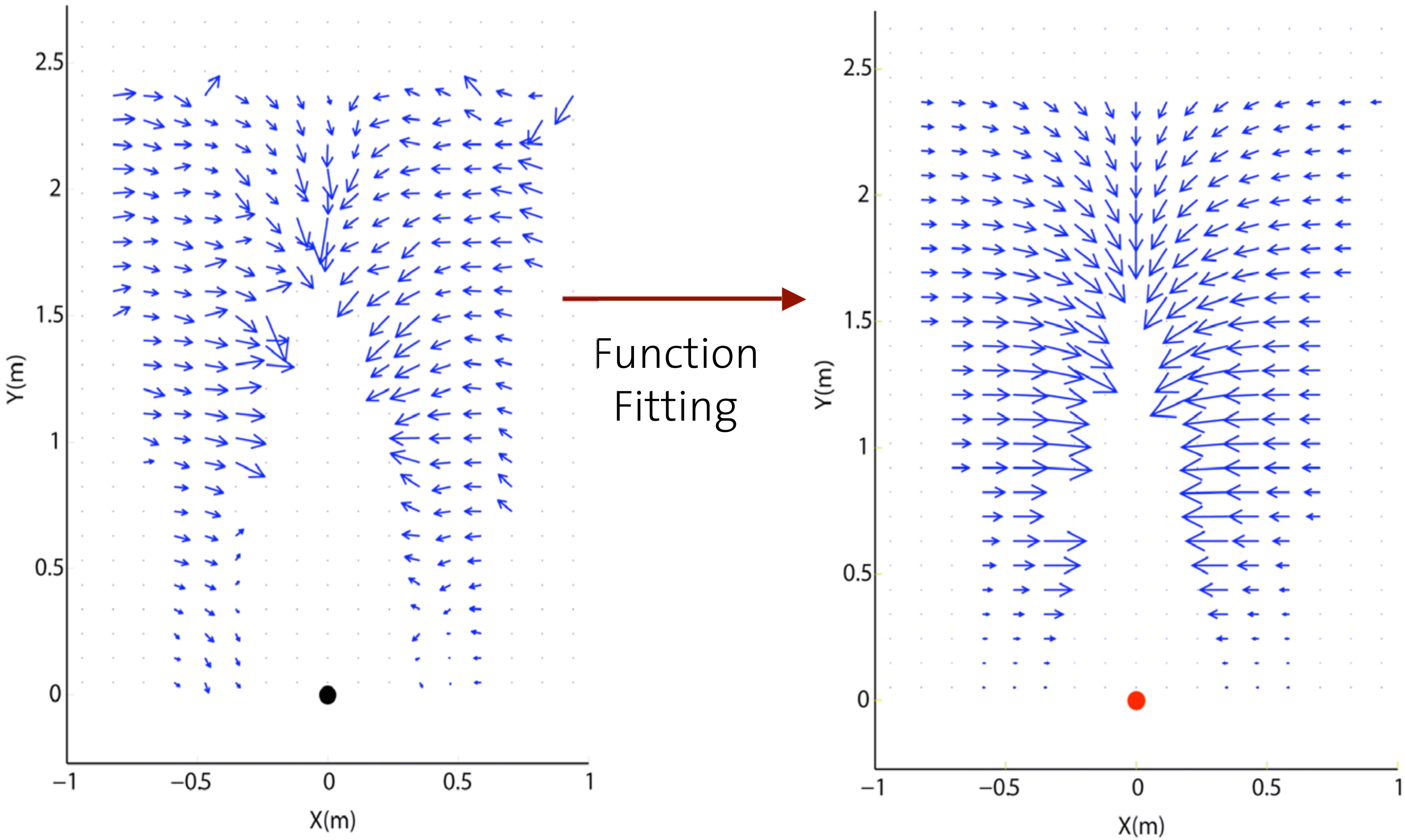

Observed

Fitted Field

Comparison of Observations and Simulations

Observation

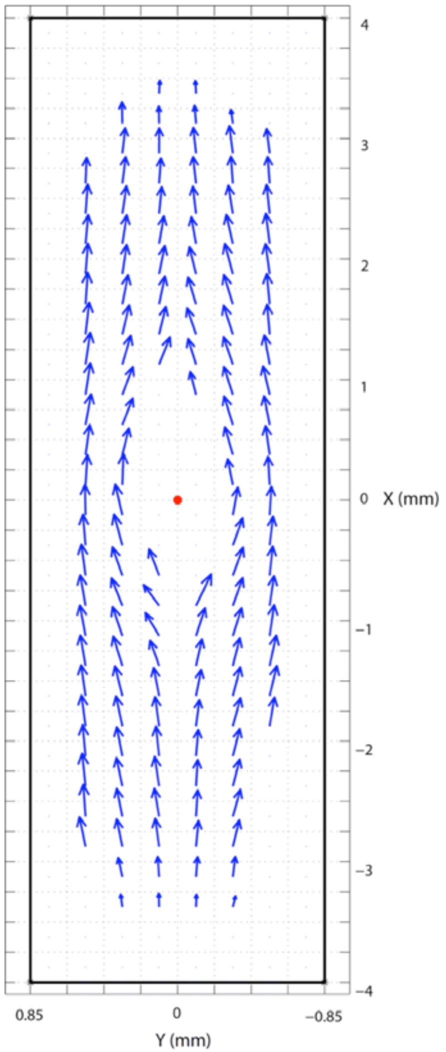

Simulation

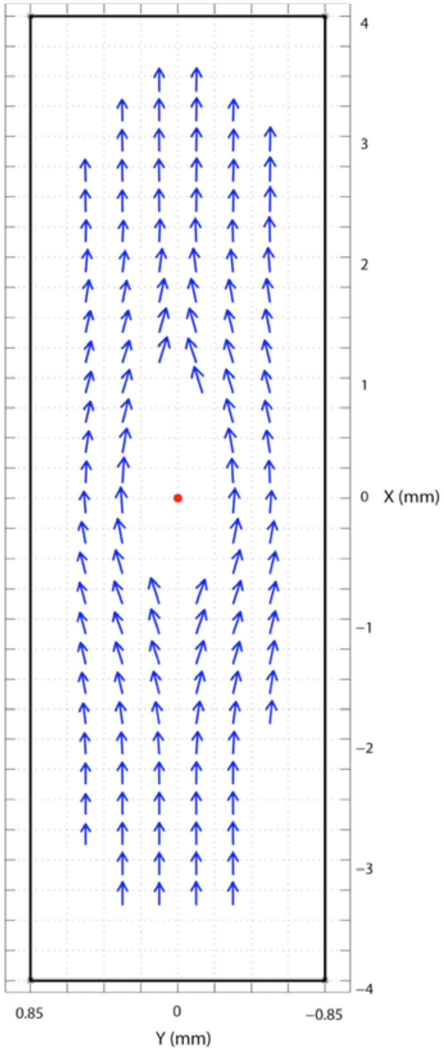

Comparison

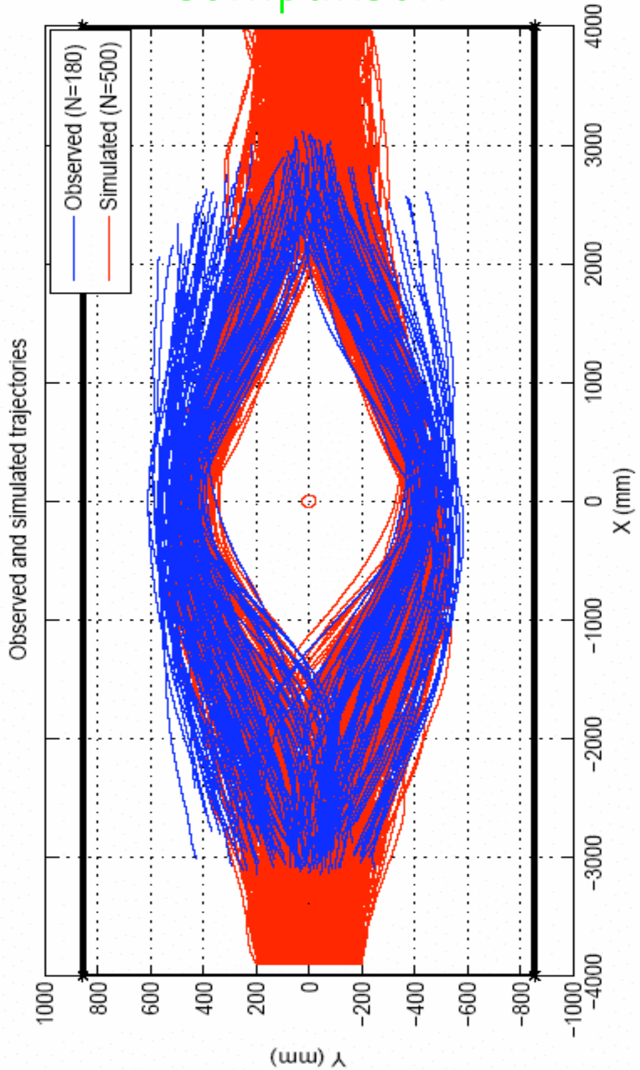

Validation 1: Corridor Experiment

- Quantitative validation

Average observed trajectory + std

Average simulated trajectory

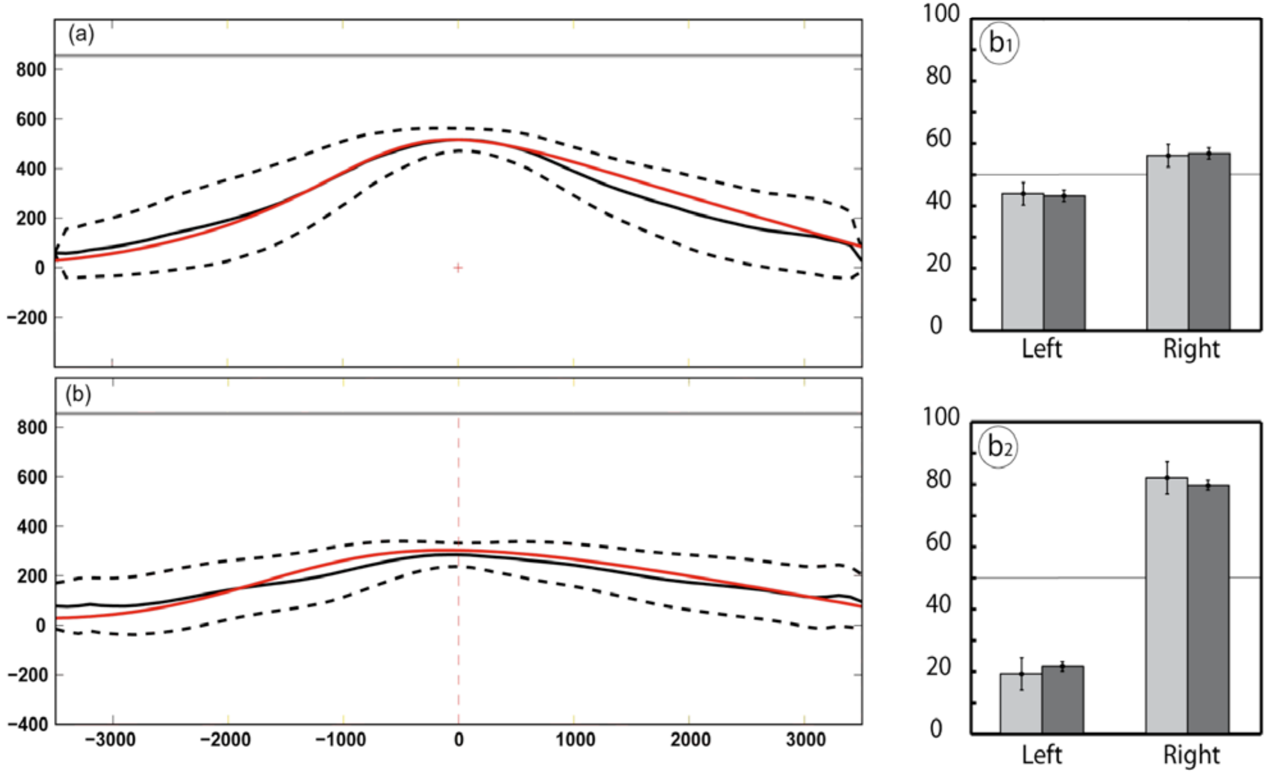

An Interactive Binary Decision Problem: Choice of Left vs. Right Side

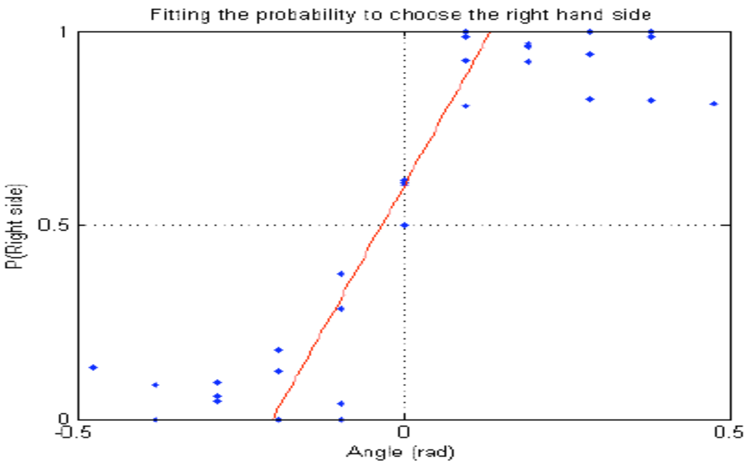

$\xi_\alpha = -1$ with probability

$$p_\alpha(\varphi) = \begin{cases} 0 & \text{if } \varphi < -0.2 \\ 0.57 + 2.85\varphi & \text{if } -0.2 \le \varphi \le 0.15 \\ 1 & \text{if } \varphi > 0.15 \end{cases}$$

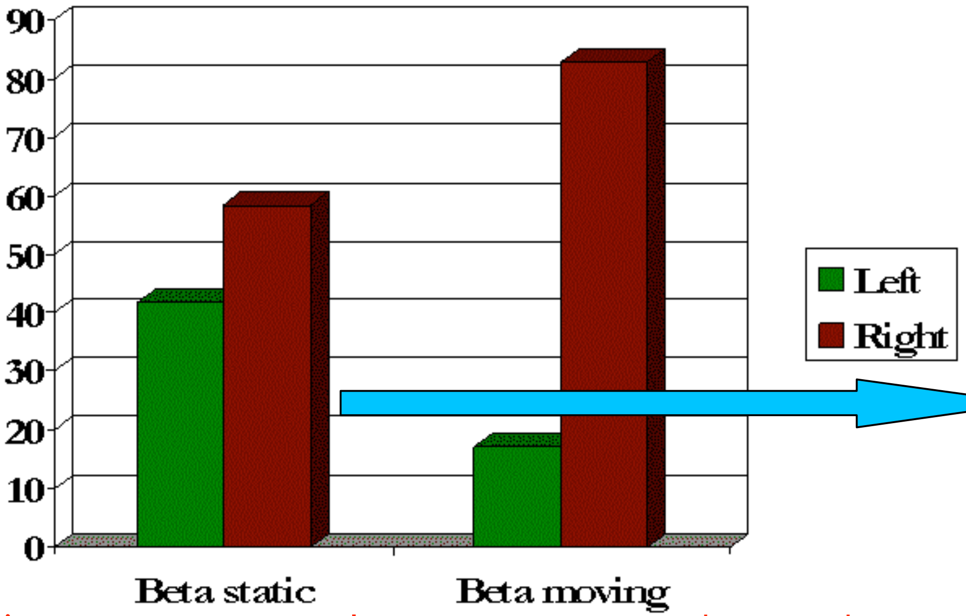

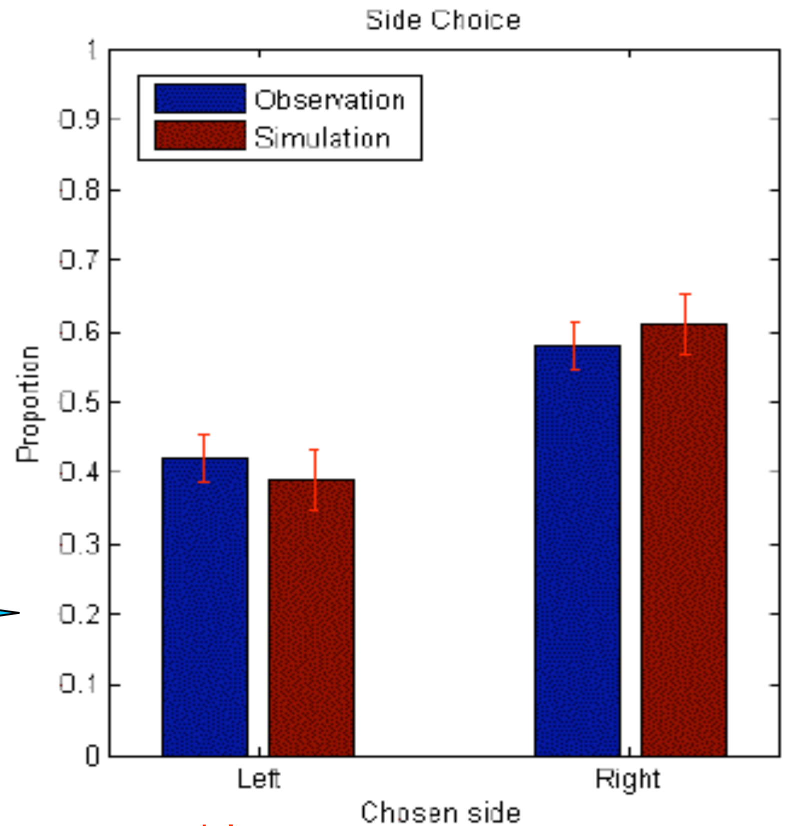

It's not just a repulsive interaction, but rather a decision problem!

Validation 2: Collective Dynamics

Observations in a crowded street

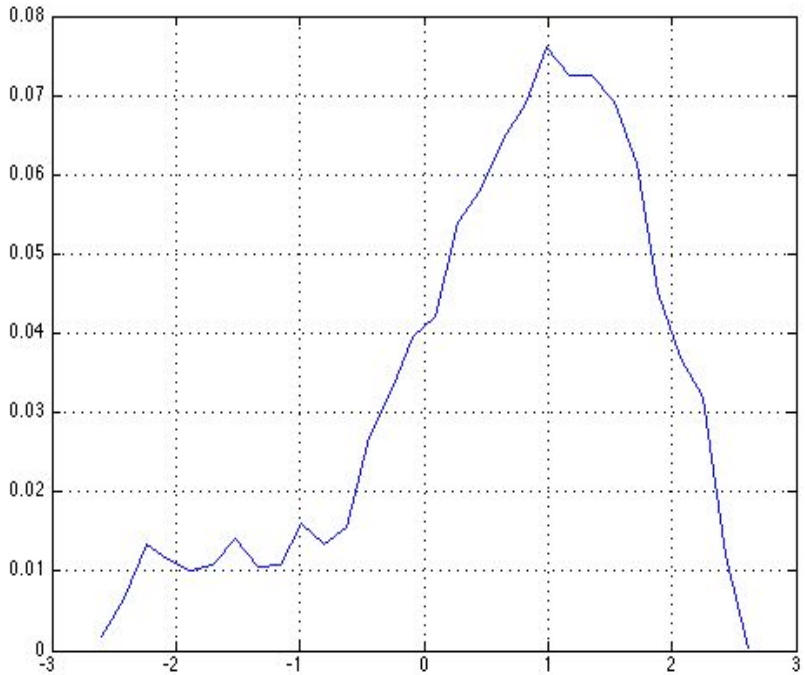

Asymmetry of flows (with respect to walking direction)

How to Optimize Pedestrian Facilities

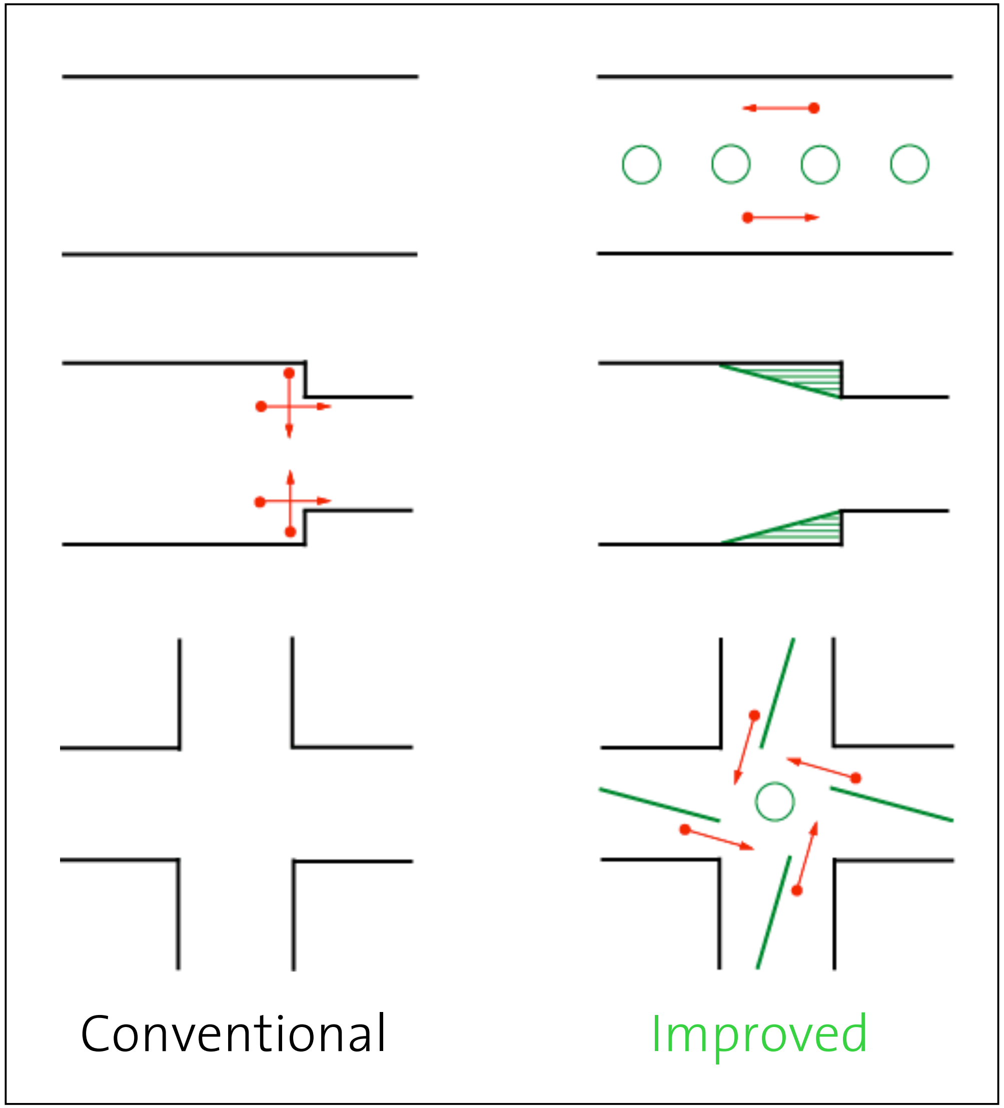

Evolutionary Optimization of Pedestrian Facilities

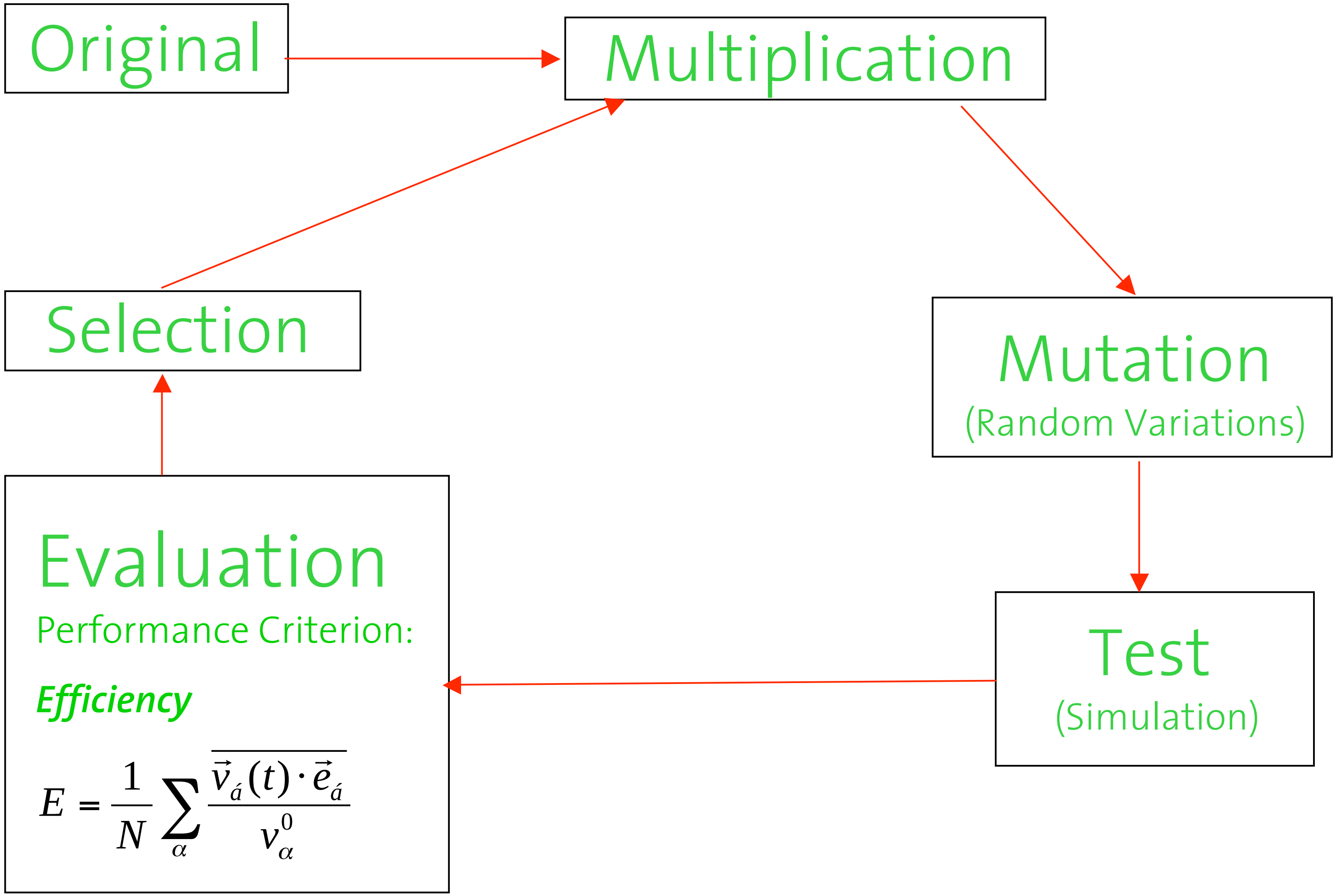

Evolutionary Optimization of a Bottleneck

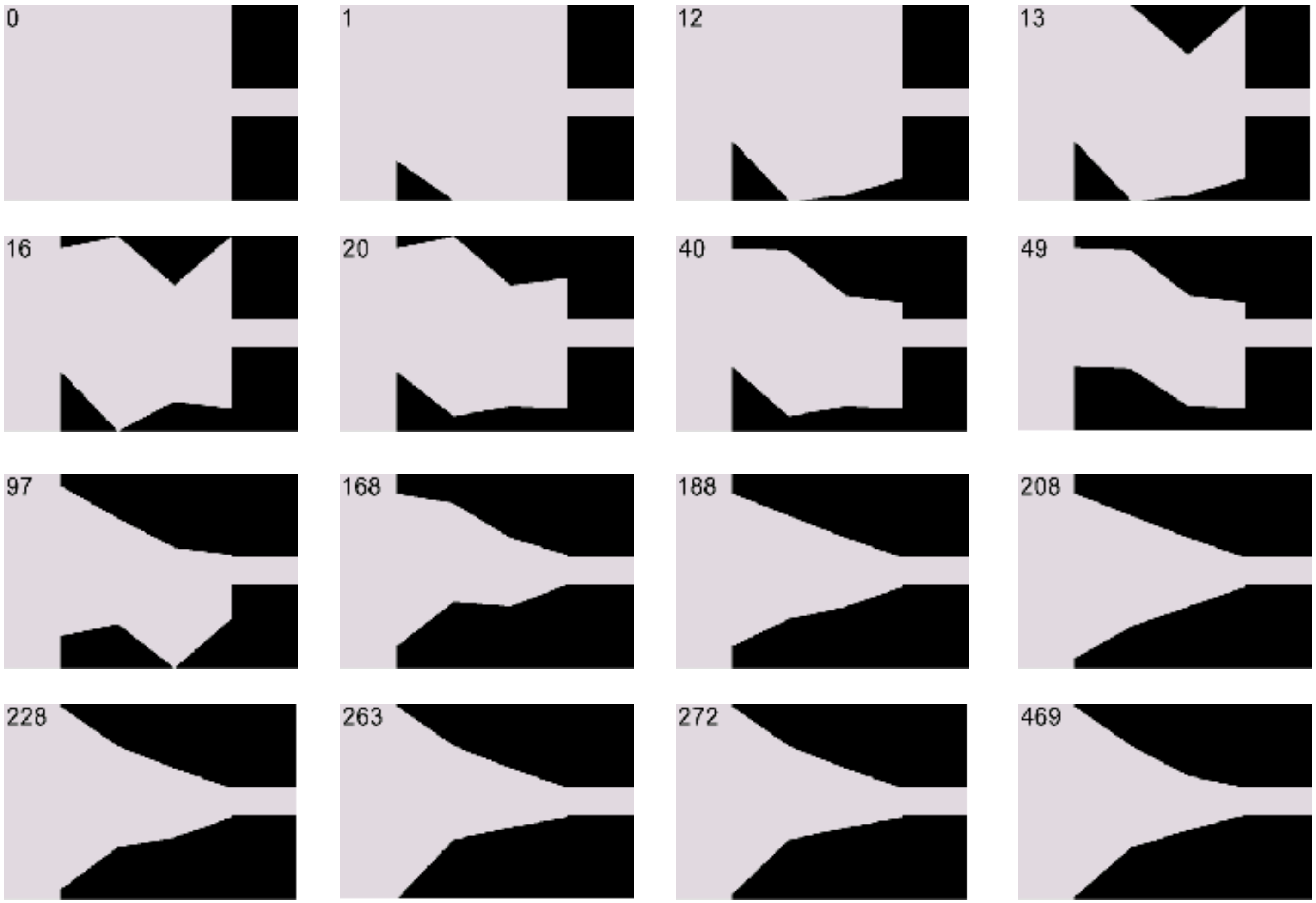

Typical Evolutionary Designs (Preliminary)

Snapshot; without obstacles

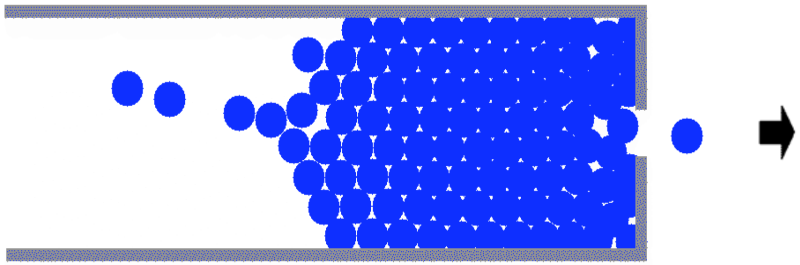

Snapshot; with obstacles

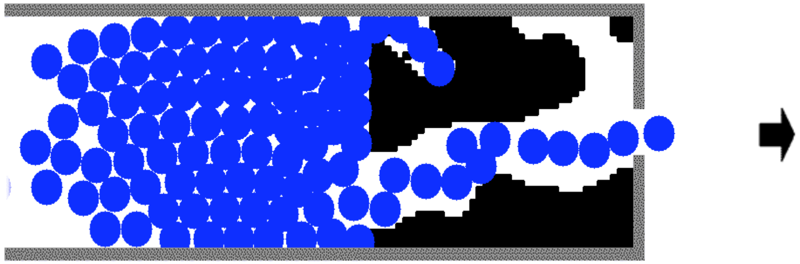

Compartment shape (fitness 0.83)

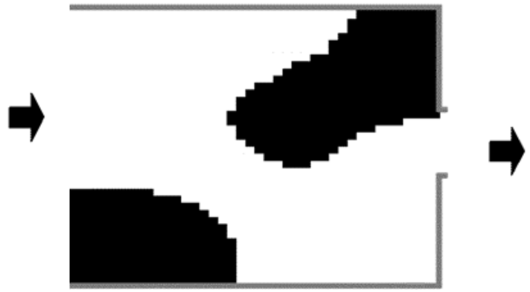

Zig-zag shape (fitness 1.78)

Funnel shape (fitness 1.99)

Self-Organization and Optimization of Intersecting Flows

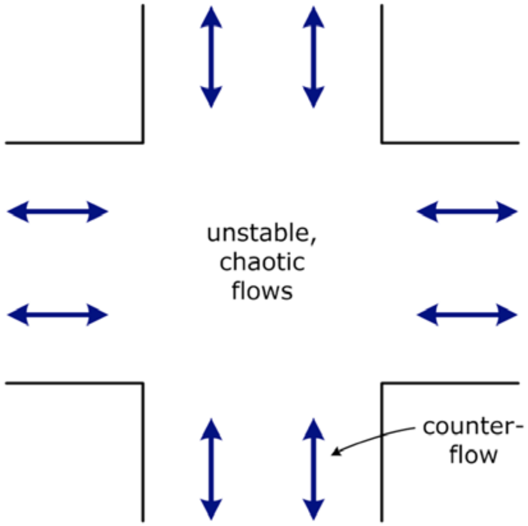

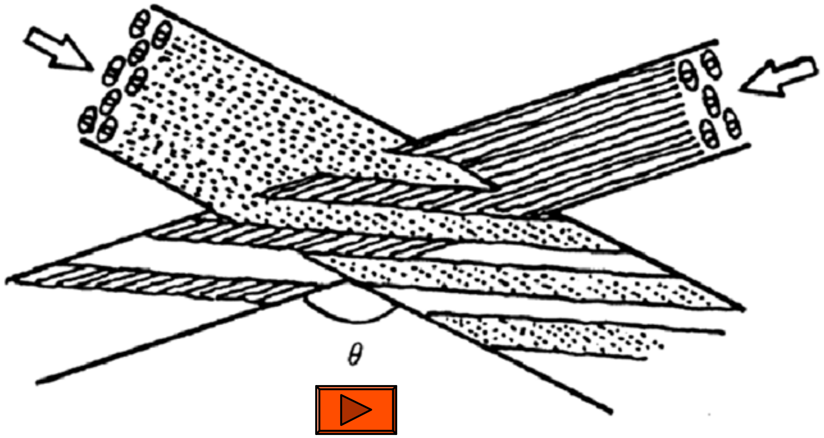

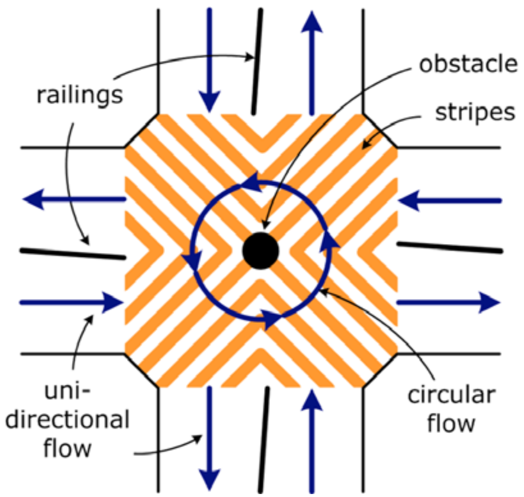

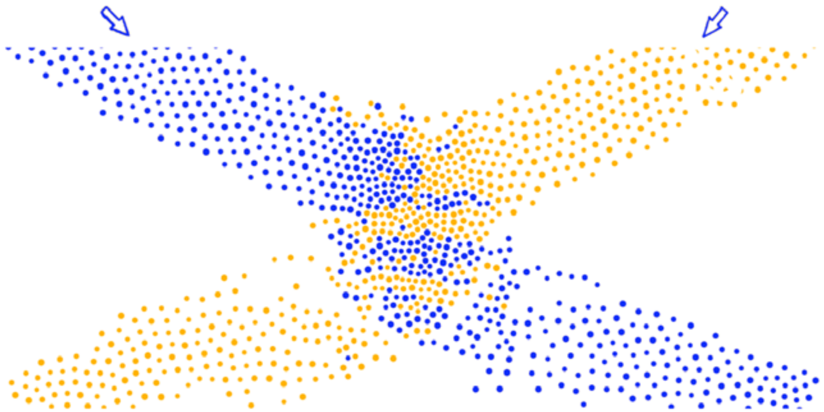

Oscillatory Flow Organization at Intersections

Practical Implications and Design Solutions for Intersections

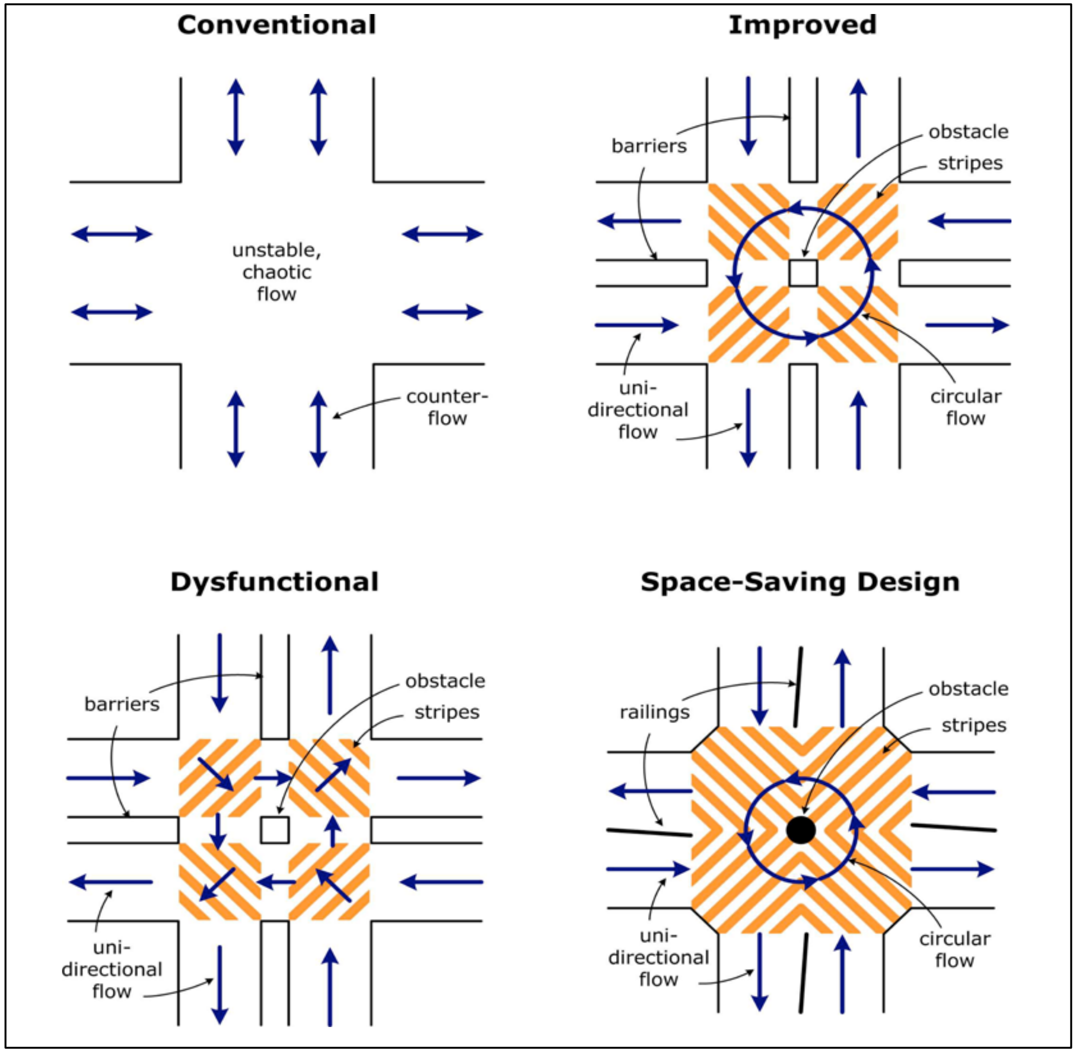

Evolutionary Pedestrian Intersection Optimization

Conventional design

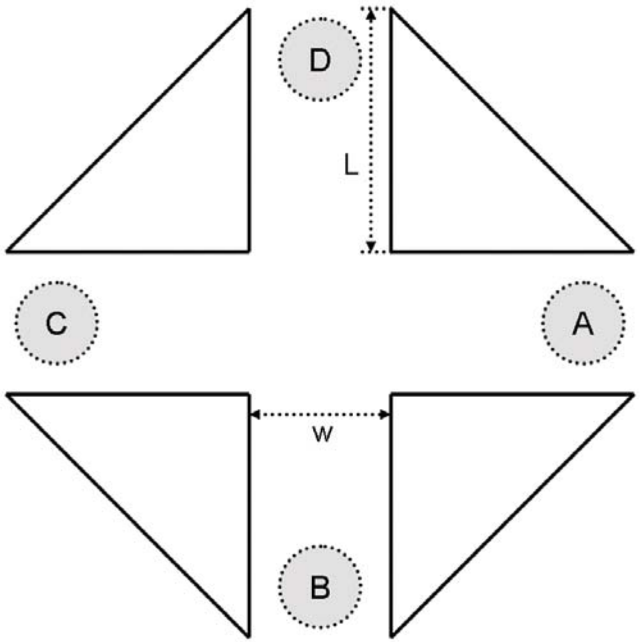

Improved design

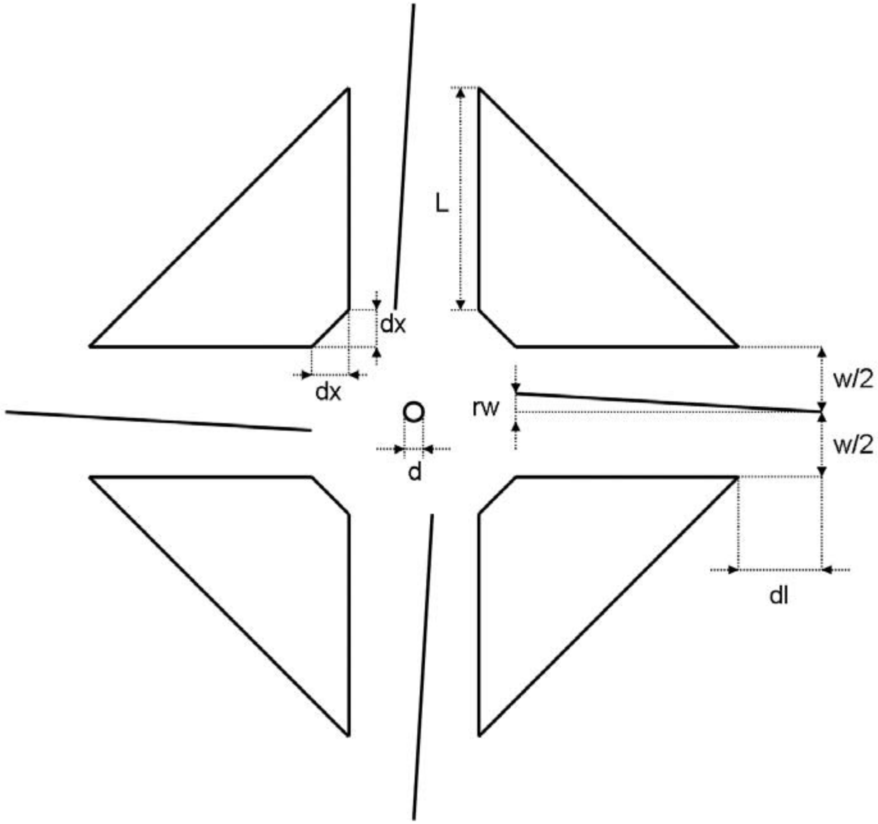

Parameters and Performance of Optimized Intersections

Pedestrian intersection optimization

A genetic algorithm was used to find the optimal values of the design and these results, compared to the conventional design:

Constant	Value	Description
L	7 m	Length of each corridor
w	2.5 m	Width of each corridor
rw	0.6 m	Transversal displacement of endpoint of of the railings
d	0.0 m	Diameter of the pillar (this pillar is not needed for the optimal flow design proposal)
dx	0.7 m	Enlargement, of each side, of the central area
dl	1.5 m	Longitudinal displacement of endpoint of of the railings
N	120	Number of pedestrians

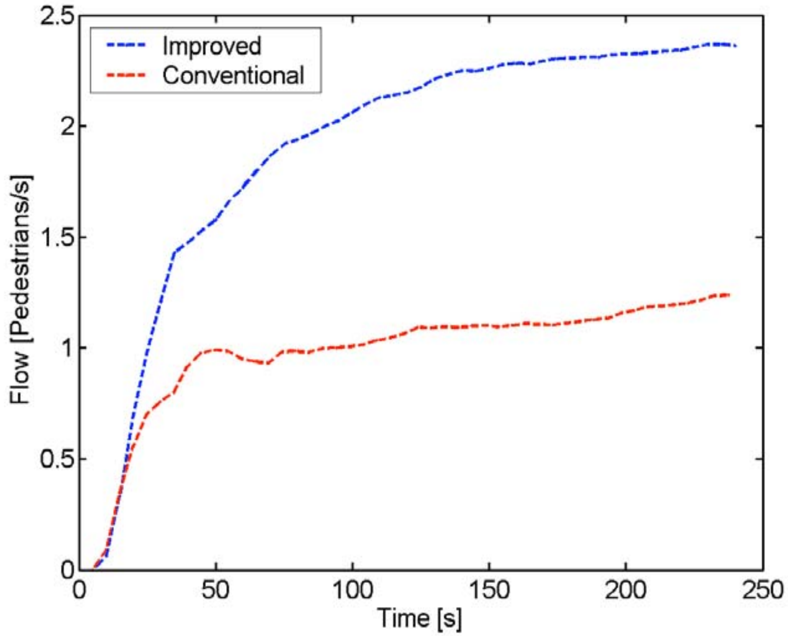

Large-Scale Simulation of Mass Events and Urban Areas

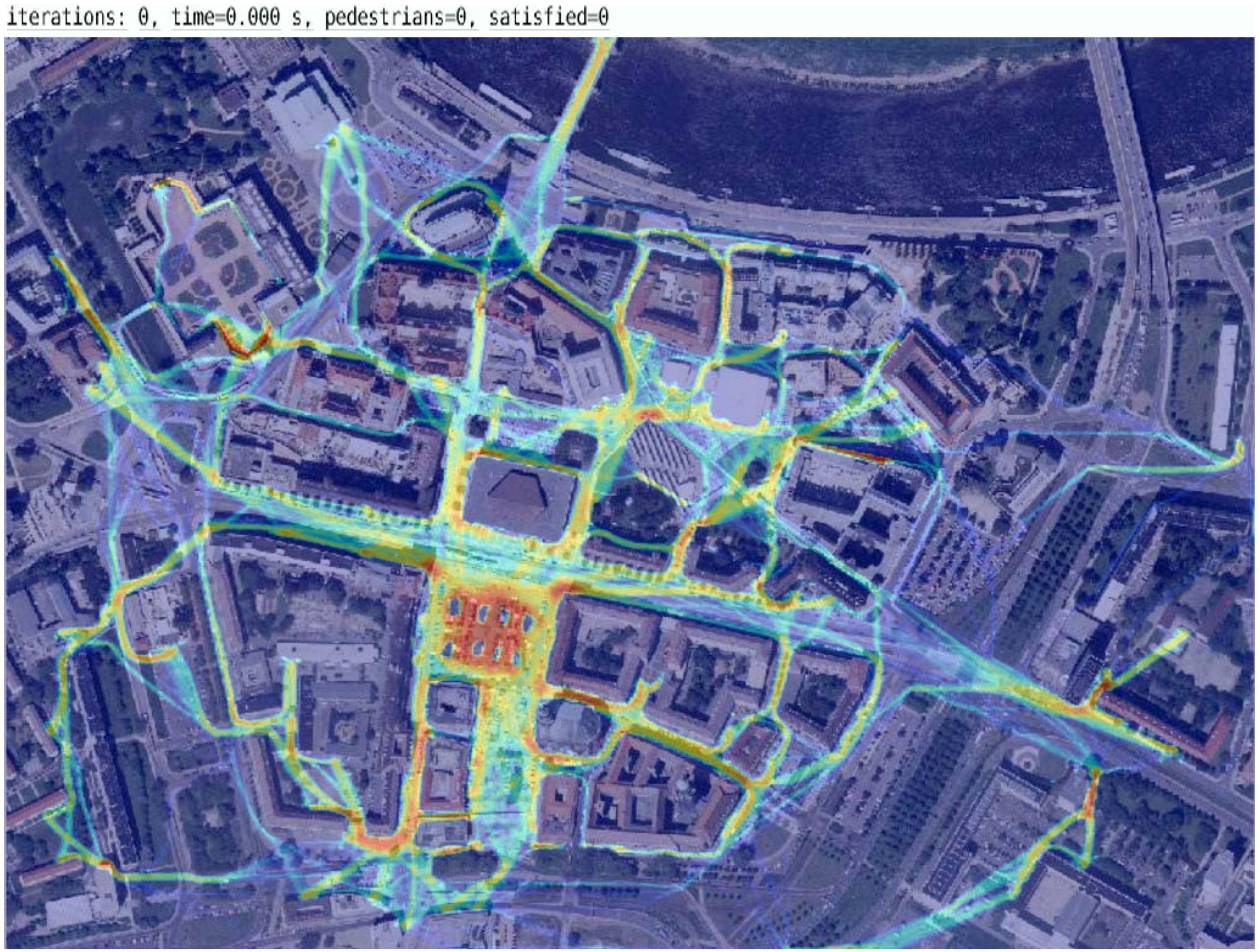

Situation of Intersecting Vehicle and Pedestrian Flows

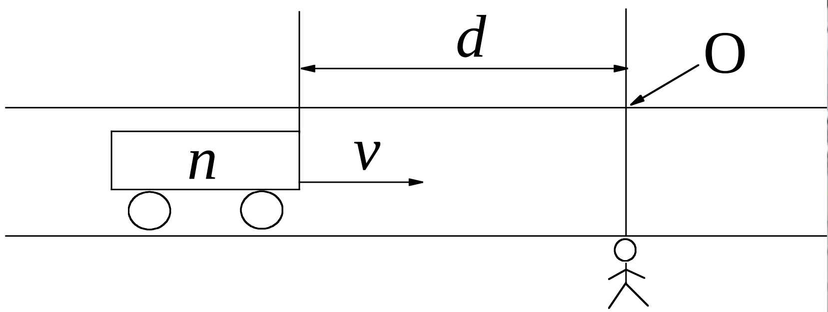

Pedestrian behavior:

We will assume that pedestrians enter the sidewalk of the street at the crossing point O with probability $p = \lambda dt$ per time step *dt* (λ denotes the arrival rate of pedestrians).

Intersecting Vehicle and Pedestrian Streams

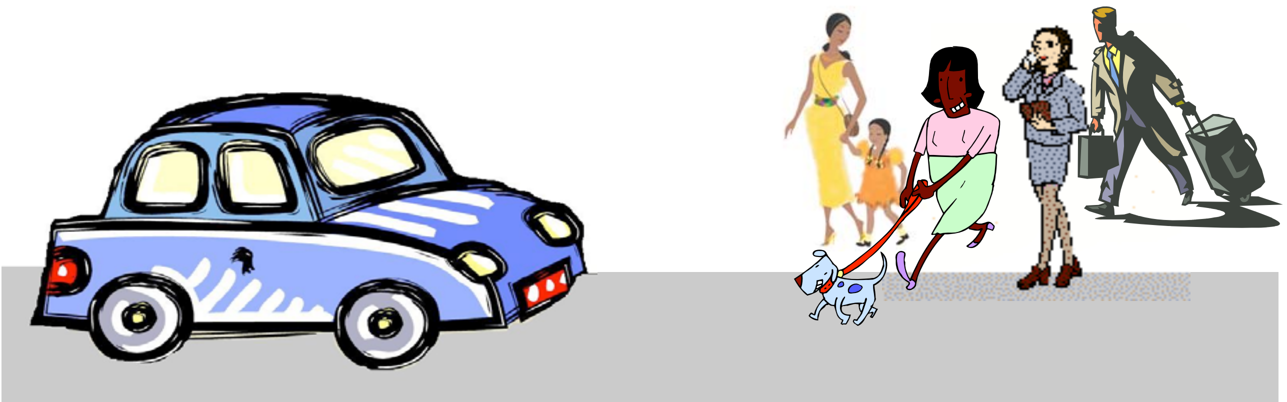

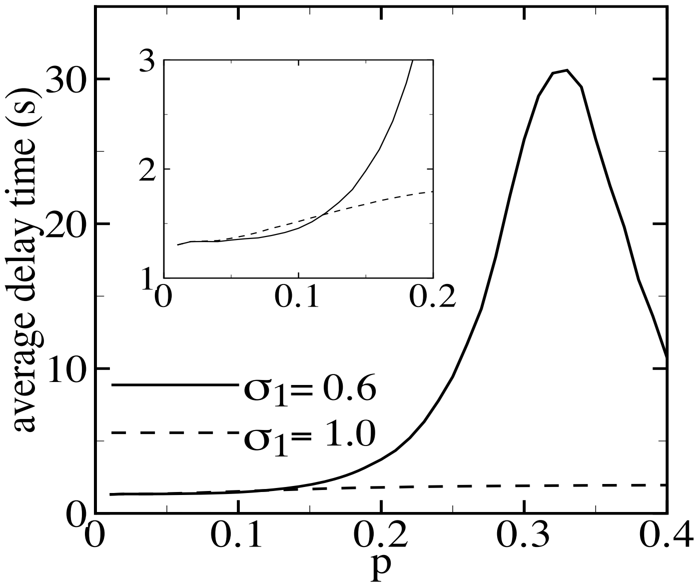

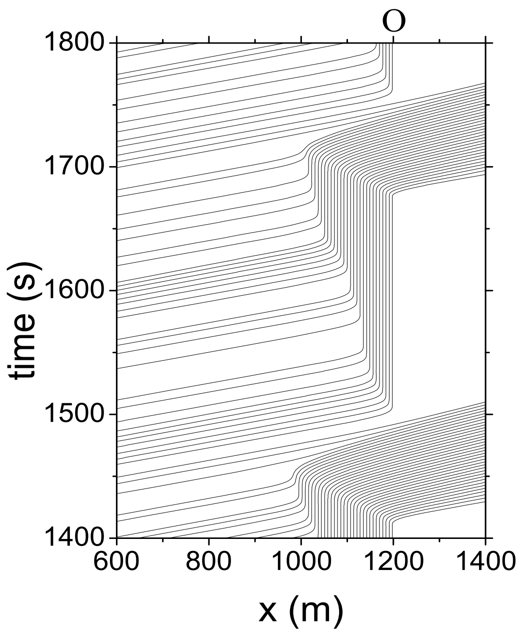

Pedestrian Behavior

If there is no sufficient gap in the vehicle stream to cross the road, pedestrians accumulate around point O, but they start immediately to enter the road at time *t*, if $v(t) = 0$(i.e. if the vehicle velocity is zero) or if

$$d(t) > d_0 \quad \text{and} \quad \Delta t(t) := \frac{d(t)}{v(t)} \geq \sigma\tau$$

Δt time to collision of the nearest approaching vehicle

σ safety factor of pedestrians

τ time period required for a pedestrian to cross (one lane of) the road.

Vehicle Behavior

The vehicle dynamics is given by a simple variant of the intelligent driver model (IDM)

$$f(\Delta x, v, v_n) = b\left[1 - \left(\frac{v_n}{v_0}\right)^4 - \left(\frac{s^*}{\Delta x}\right)^3\right]$$

$$s^* = s_0 + T v_n + \frac{v_n(v_n - v_{n-1})}{2b}$$

For the nearest vehicle *n* upstream of the crossing point O,

if a pedestrian is on the street, we have

$$\Delta x(t) = d(t) = x_O - x_n(t)$$

and

$$v_{n-1} = 0$$

Simulation Result: "Faster-is-Slower Effect"

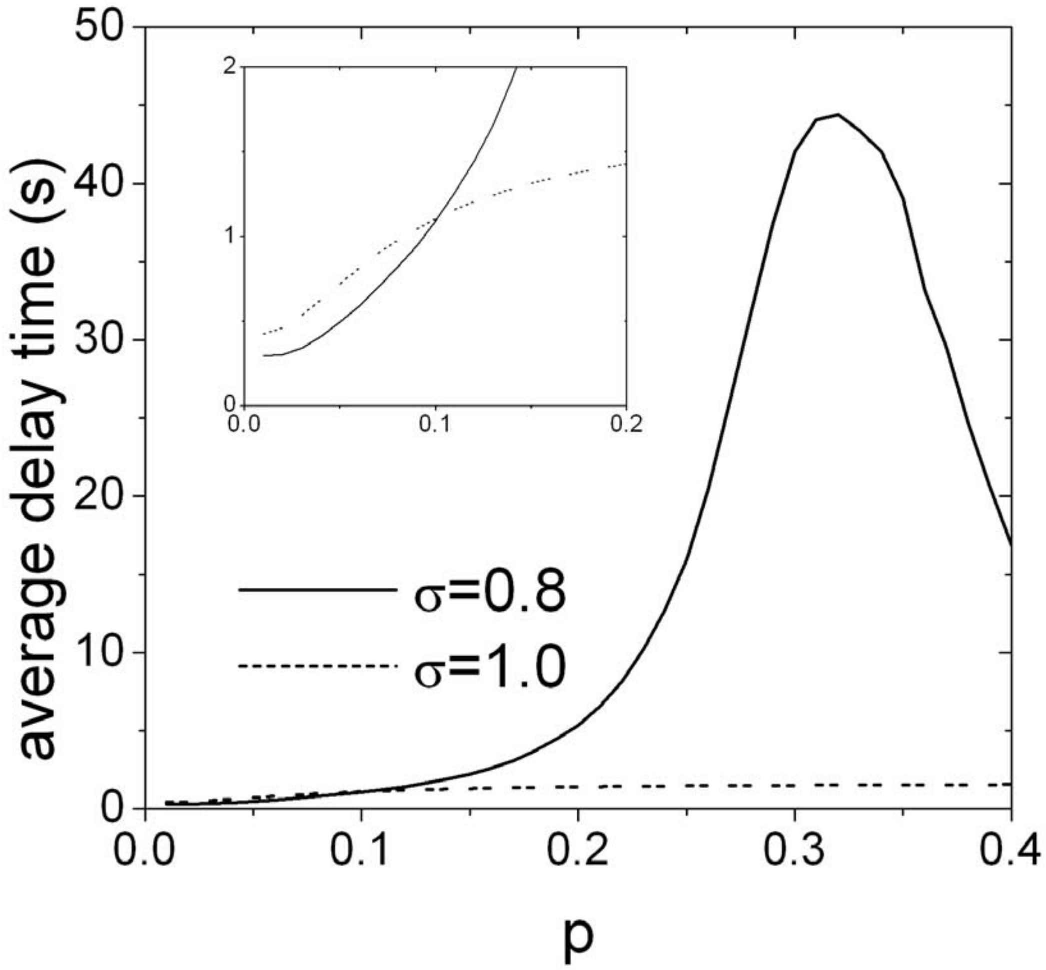

Average delay to pedestrians

Simulation Results: Underlying Dynamics

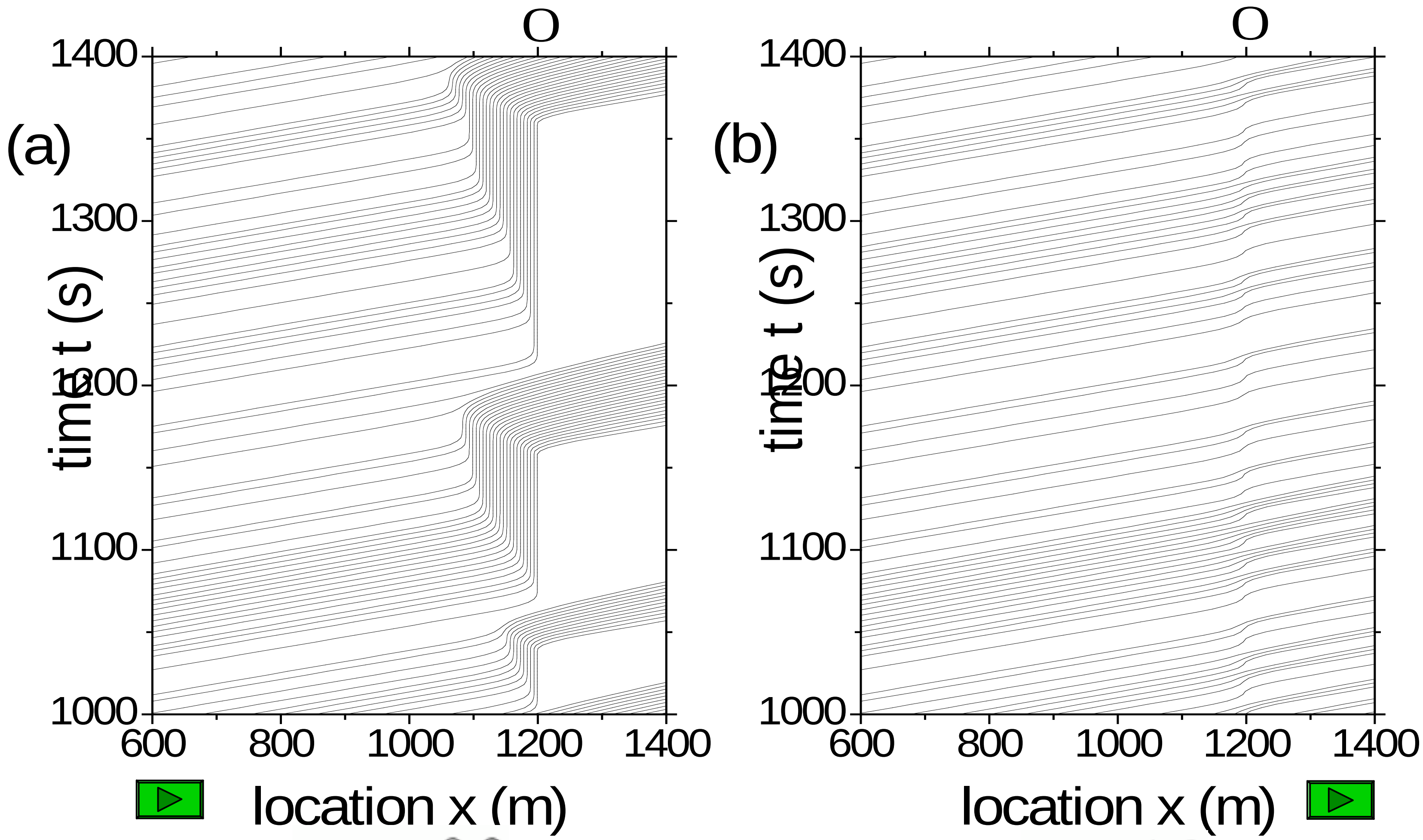

$\sigma = 0.8$ $\qquad$ $\sigma = 1.0$

Representative space-over-time plots of vehicle trajectories

Human Trail Formation

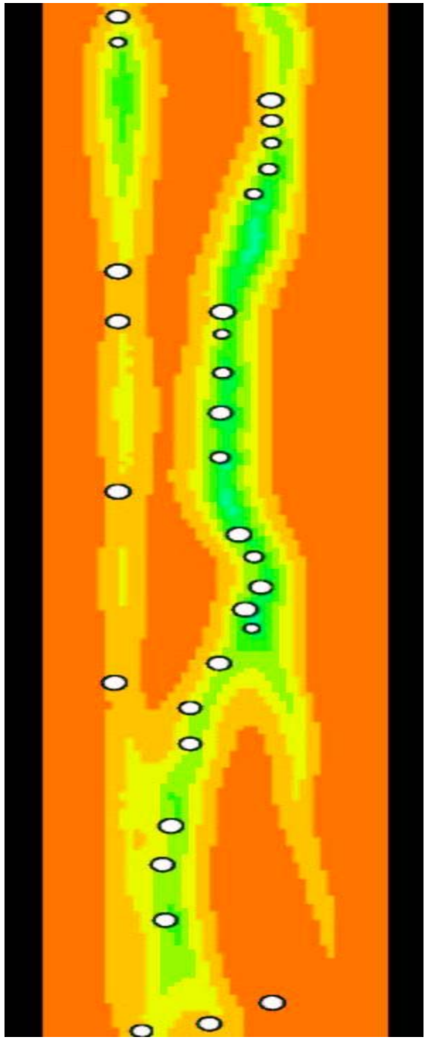

Mechanism of Trail Bundling

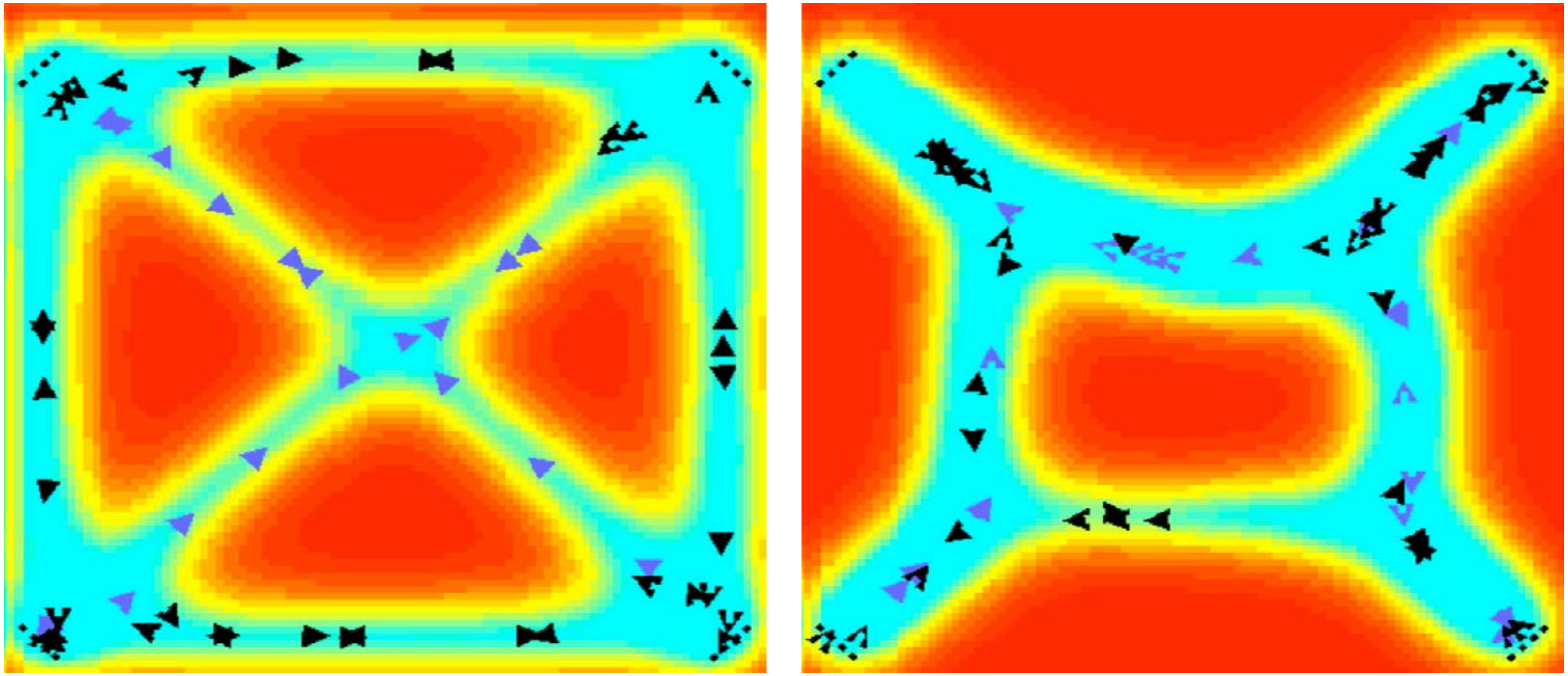

Fair solution, 22% detour for every-one, in contrast to minimal graphs

Y-Junctions Are Preferable to T-Junctions